



Systematic Review

Cingulum and Uncinate Fasciculus Microstructural Abnormalities in Parkinson's Disease: A Systematic Review of Diffusion Tensor Imaging Studies

Fatemeh Rashidi ¹, Mohammad Hossein Khanmirzaei ¹, Farbod Hosseinzadeh ¹, Zahra Kolahchi ¹, Niloofar Jafarimehrabady ², Bardia Moghisseh ³  and Mohammad Hadi Aarabi ^{4,*} 

¹ School of Medicine, Tehran University of Medical Science, Tehran 1417613151, Iran

² Department of Clinical-Surgical, Diagnostic and Pediatric Sciences, University of Pavia, 27100 Pavia, Italy

³ School of Medicine, Arak University of Medical Science, Arak 3848176941, Iran

⁴ Department of Neuroscience (DNS), Padova Neuroscience Center, University of Padova, 35128 Padua, Italy

* Correspondence: mohammadhadiarabi@gmail.com; Tel.: +39-347-831-1484

Simple Summary: This article reviews the use of diffusion tensor imaging (DTI) to evaluate changes in white matter microstructure within two specific fiber tracts in Parkinson's disease patients. It also examines how these structural changes may be related to cognitive impairments seen in advanced PD patients and provides insight into developing more targeted treatments for different types of Parkinson's disease.

Abstract: Diffusion tensor imaging (DTI) is gaining traction in neuroscience research as a tool for evaluating neural fibers. The technique can be used to assess white matter (WM) microstructure in neurodegenerative disorders, including Parkinson disease (PD). There is evidence that the uncinate fasciculus and the cingulum bundle are involved in the pathogenesis of PD. These fasciculus and bundle alterations correlate with the symptoms and stages of PD. PRISMA 2022 was used to search PubMed and Scopus for relevant articles. Our search revealed 759 articles. Following screening of titles and abstracts, a full-text review, and implementing the inclusion criteria, 62 papers were selected for synthesis. According to the review of selected studies, WM integrity in the uncinate fasciculus and cingulum bundles can vary according to symptoms and stages of Parkinson disease. This article provides structural insight into the heterogeneous PD subtypes according to their cingulate bundle and uncinate fasciculus changes. It also examines if there is any correlation between these brain structures' structural changes with cognitive impairment or depression scales like Geriatric Depression Scale-Short (GDS). The results showed significantly lower fractional anisotropy values in the cingulum bundle compared to healthy controls as well as significant correlations between FA and GDS scores for both left and right uncinate fasciculus regions suggesting that structural damage from disease progression may be linked to cognitive impairments seen in advanced PD patients. This review help in developing more targeted treatments for different types of Parkinson's disease, as well as providing a better understanding of how cognitive impairments may be related to these structural changes. Additionally, using DTI scans can provide clinicians with valuable information about white matter tracts which is useful for diagnosing and monitoring disease progression over time.

Keywords: diffusion tensor imaging (DTI); Parkinson disease (PD); cingulum; uncinate fasciculus; non-motor symptoms; motor symptoms



Citation: Rashidi, F.; Khanmirzaei, M.H.; Hosseinzadeh, F.; Kolahchi, Z.; Jafarimehrabady, N.; Moghisseh, B.; Aarabi, M.H. Cingulum and Uncinate Fasciculus Microstructural Abnormalities in Parkinson's Disease: A Systematic Review of Diffusion Tensor Imaging Studies. *Biology* **2023**, *12*, 475. <https://doi.org/10.3390/biology12030475>

Academic Editor: Anne Beck

Received: 16 February 2023

Revised: 12 March 2023

Accepted: 15 March 2023

Published: 20 March 2023



Copyright: © 2023 by the authors. Licensee MDPI, Basel, Switzerland. This article is an open access article distributed under the terms and conditions of the Creative Commons Attribution (CC BY) license (<https://creativecommons.org/licenses/by/4.0/>).

1. Introduction

Parkinson's disease (PD) is a prevalent neurodegenerative disorder that affects 1% of individuals over the age of 60 worldwide [1–3]. Symptoms of PD can be divided into two categories: motor and nonmotor. Motor symptoms, which are the most well known, include akinesia (reduced movement), bradykinesia (slowness of movement), tremor, rigidity, gait

disturbance, and speech deficits [4]. In recent years, nonmotor symptoms of PD have received increased attention. These symptoms include autonomic dysfunction, sensory issues, cognitive impairment, sleep disturbances, apathy, depression, and anxiety [5,6]. From a pathophysiological perspective, it is believed that these symptoms result from the loss, degeneration, and impaired neurogenesis of dopaminergic neurons in specific regions of the brain, such as the basal ganglia, the substantia nigra, the hippocampus, the limbic system, and the white matter [7–10].

Studies utilizing diffusion tensor imaging (DTI) on animal models of Parkinson's disease induced by toxins, resulting in the loss of dopaminergic neurons in the substantia nigra (SN), have yielded inconclusive results regarding changes in DTI measures [11,12].

White matter (WM) degeneration is a commonly observed magnetic resonance imaging (MRI) finding in PD, and it is characterized by abnormal fiber connections in the brain. This degeneration can affect various regions of the brain, including the prefrontal limbic system. This degeneration might also lead to the cognitive impairment and changes in emotion regulation often seen in PD patients [13,14]. Abnormal white matter fibers have been suggested as a potential cause of depression in PD. The limbic system, a complex of brain structures that plays significant roles in memory, language, goal-directed behavior, affective behavior, and emotional behavior, is also affected in PD. The limbic system includes structures such as the cingulate gyrus, hippocampus, parahippocampal gyrus, amygdala, mammillary bodies, hypothalamus, and the nucleus accumbens [15,16]. The uncinate fasciculus (Figure 1), which connects the inferior frontal gyrus with the anterior temporal lobe regions, is traditionally a considered part of the limbic system [17]. The cingulum (Figure 1), a bundle of nerve fibers that runs from the orbital frontal cortex, along the corpus callosum's dorsal surface, and down the temporal lobe, is also an integral part of the limbic system [18,19].

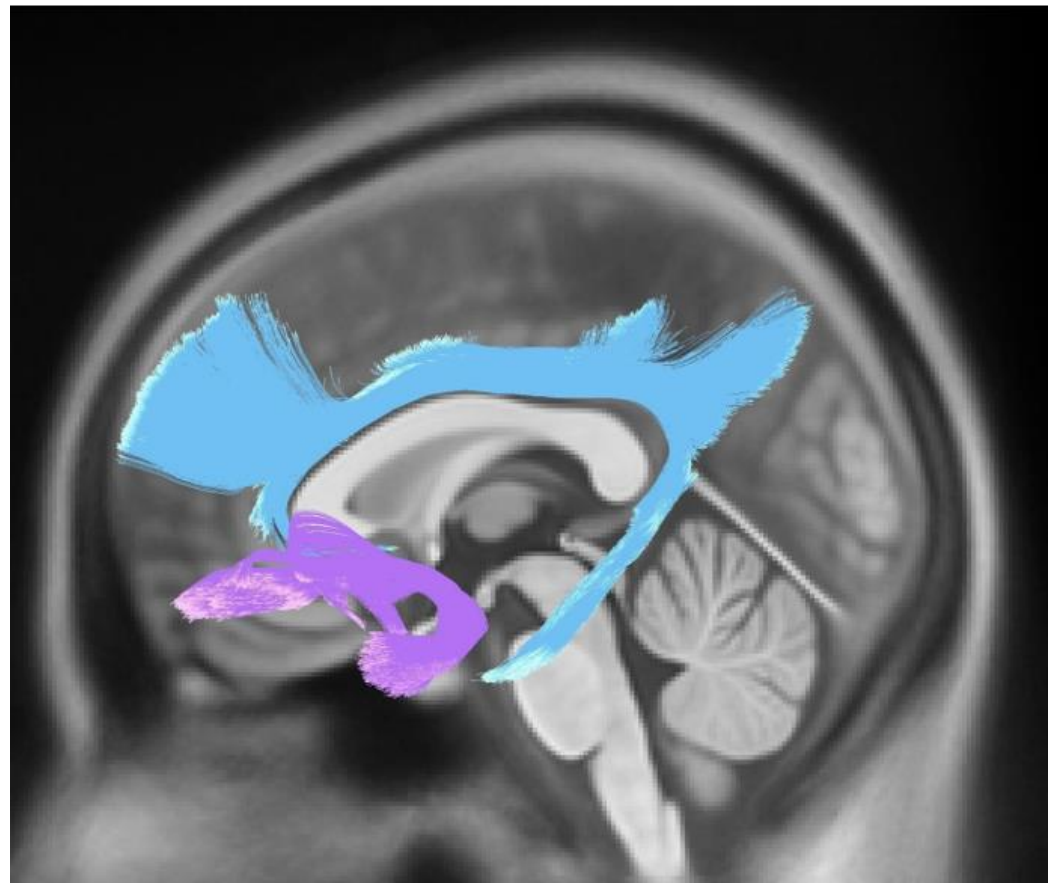


Figure 1. Tractography of cingulum (blue) and uncinate fasciculus (purple).

Recent MRI studies have revealed dysfunction of the cingulum in a variety of neurological and psychiatric disorders. Despite limited available data on anatomy and function of the cingulum, it is crucial to unravel hidden interactions of the highly complex limbic system [20]. DTI is a technique used to assess the microstructural composition of white matter by analyzing the movement of water molecules in the brain. It has been used to detect changes in the brain tissue caused by neurological diseases [21]. Intact WM contributes to high fractional anisotropy (FA), which results from high directionality of water diffusion along axon bundles and lower tissue density [22]. Mean diffusivity (MD) is also used to assess the diffusion of water [23]. Additionally, diffusion can be measured parallel or perpendicular to white matter fascicles, known as axial diffusivity (AD) and radial diffusivity (RD), respectively. Changes in AD values indicate axonal damage and fragmentation, while changes in RD values indicate changes in axonal density, axonal diameter, and myelination [23].

DTI has been widely used to investigate pathological changes in the WM of PD patients by probing the diffusivity of water molecules within the WM tracts [24].

In this systematic review, we aim to provide a comprehensive understanding of specific WM fiber tracts, particularly the cingulum bundle and uncinate fasciculus, in Parkinson's disease patients, in terms of their associations with DTI profiles.

2. Search Strategy and Data Extraction

We performed a systematic search of the published literature to identify the studies that investigated the involvement of uncinate fasciculus and cingulum associated with PD pathology and symptomatology using DTI. We used the broad search terms: "Diffusion Tensor imaging" [All Fields] OR "Diffusion tensor MRI" [All Fields] OR "Diffusion MRI" [All Fields] OR "DTI" [All Fields] AND ("Parkinson's disease" [All Fields] OR "Parkinson disease" [All Fields] OR "PD" [All Fields]). We searched electronic databases including Scopus and PubMed from 2015 to November 2022. This was complemented by manual searching of the related papers through the list of references. To avoid duplication, the results were imported to Covidence software and articles were separately screened by two of the authors (Z.K. and M.H.K.). In case of disagreement, a third person (F.H.) interfered to decide whether to include or exclude articles. Among the search results, abstracts were screened for relevance. Studies which had investigated diseases other than PD or had used imaging methods other than DTI were excluded. Full papers were obtained for studies published in English that performed DTI in PD patients, and further assessed if they had investigated the cingulate bundle and uncinate fasciculus in PD patients to be included in this systematic review. Figure 2 illustrates the process of study selection according to the PRISMA guidelines.

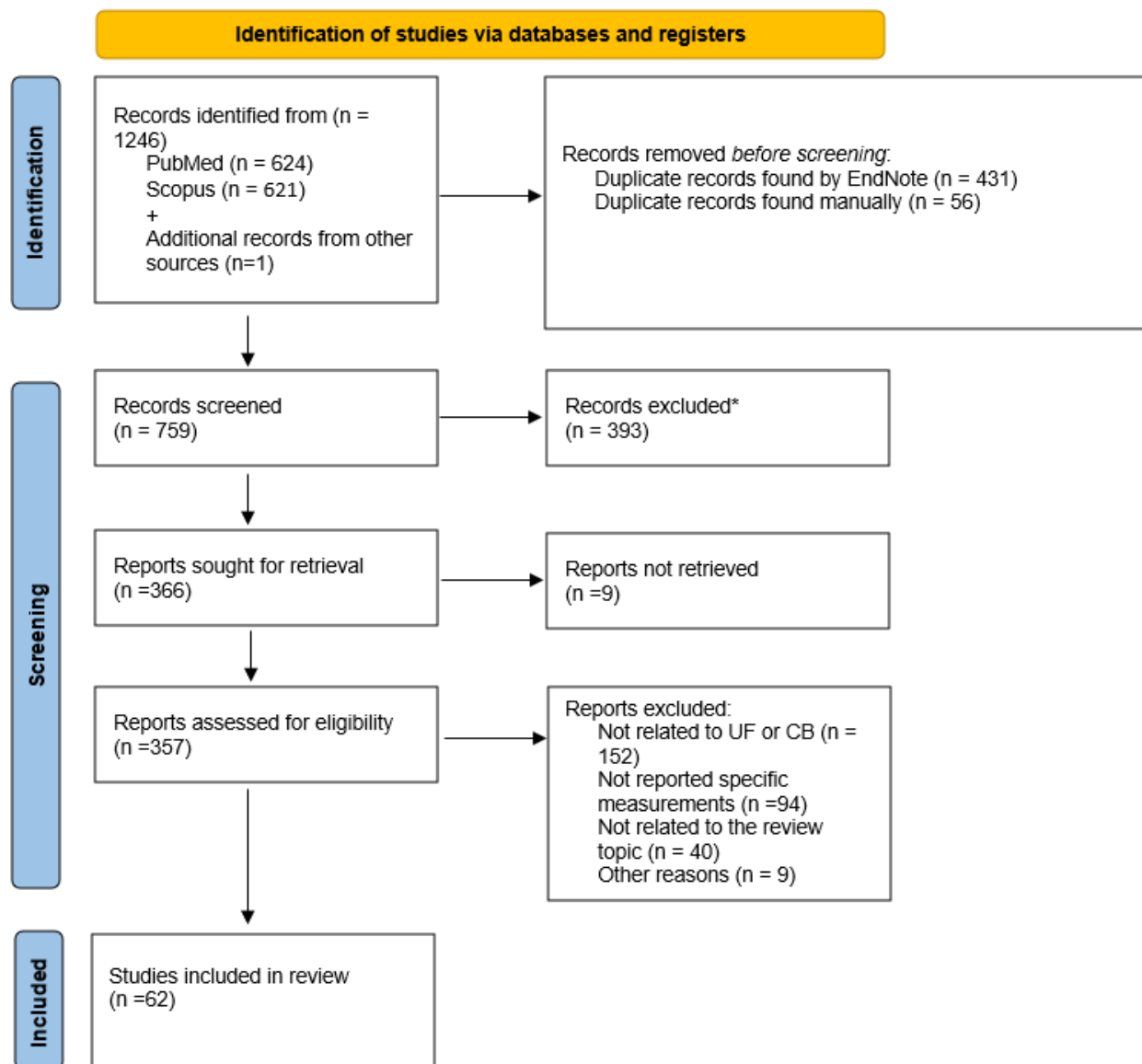


Figure 2. PRISMA flow diagram for DTI of the cingulum and uncinate fasciculus in PD. *, studies which had investigated diseases other than PD or had used imaging methods other than DTI were excluded.

3. Result

In our literature review, we identified 61 studies that investigated the changes in the uncinate fasciculus and cingulum in PD and used the PRISMA guidelines. One additional study was found during the writing process [25].

The studies were conducted globally, with inclusion ranging from 2015 until December 2022. However, several studies examining white matter changes in PD patients were excluded as they were either animal studies. Additionally, any studies that focused on structures other than the uncinate fasciculus and cingulum were also excluded. A summary of the study demographics is presented in Table 1.

Table 1. An overview of the demographic of literature regarding studies with significant microstructural changes of Cingulum and Uncinate Fasciculus in association with PD symptoms.

Demographic Features				
Study	Groups Studied	Number of Participants (Male)	Mean Age \pm SD (Years) or Range	Disease Duration \pm SD (Years) or Range
Boyu Chen et al., 2015 [26]	HC	21 (11)	61.10 \pm 8.336	–
	PD-Cu	19 (10)	59.47 \pm 8.771	3.21 \pm 1.960
	PDD	11 (6)	64.09 \pm 11.353	3.64 \pm 2.693
Zonghong Li et al., 2020 [27]	HC	91 (40)	57.67 \pm 5.27	–
	non-depressed PD	43 (24)	58.09 \pm 6.52	6.28 \pm 3.38
	depressed PD	30 (13)	59.23 \pm 7.10	5.46 \pm 4.25
Florian Holtbernd et al., 2019 [28]	PD	29 (21)	63.5 \pm 8.3	80.9 \pm 85.7 (months)
	HC	56 (42)	62.9 \pm 11.0	–
	RBD	30 (29)	66.8 \pm 9.1	121.0 \pm 162.4
Martin Gorges et al., 2019 [29]	HC	72 (39)	65 \pm 7	9 \pm 4
	PD	134 (98)	67 \pm 8	9 \pm 5
Junyan Sun et al., 2021 [30]	PD	68 (36)	58.94 (8.969)	–
	HC	77 (30)	59.58 (8.537)	4 (0.5–20)
Mattis Jalakas et al., 2019 [31]	HC	51 (0.56) (1 = female)	65 (8.5)	NA
	PD	175 (0.37)	65 (10)	5.1 (4.9)
	PDD	30 (0.3)	72.5 (6.6)	14 (6.8)
Christina Andica et al., 2019 [32]	HC	20 (12)	67.15 1.18	–
	PD	20 (11)	65.05 10.9	6.95 3.93
Christina Andica et al., 2020 [33]	HC	25 (10)	67.88 \pm 2.11	–
	PD-woNCP	19 (6)	67.21 \pm 8.16	9.84 \pm 6.21
	PD-wNCP	20 (12)	70.15 \pm 4.03	9.95 \pm 7.69
Nan-Kuei Chen et al., 2018 [34]	PD	7 (0)	64.03–10.30	62.9–43.6 (months)
	HC	15 (0)	58.03–9.28	–
Haruka Takeshige-Amano et al., 2022 [35]	HC	20 (9)	66.75 1.07	–
	PD-ICB	19 (10)	67.11 7.00	14.3 7.75
	PD-nICB	18 (5)	66.28 5.03	10.2 4.82
Jia-Yong Wu et al., 2017 [36]	PDD	31 (18)	58.8 \pm 8.67	3.23 \pm 3.04
	PDnD	37 (23)	59.1 \pm 11.4	2.40 \pm 2.53
Jingwen Chen et al., 2022 [37]	HC	50 (28)	59.2 \pm 6.3	–
	LAR	38 (17)	59.4 \pm 10.3	4.5 \pm 4.5
	LTD	32 (16)	60.4 \pm 8.9	3.9 \pm 3.1
	RAR	43 (25)	57.9 \pm 10.6	3.4 \pm 3.2
	RTD	48 (34)	59.3 \pm 9.7	4.5 \pm 4.2
Sonia Di Tella et al., 2020 [38]	HC	17 (9)	64.08 (12.71)	NA
	PD	19 (10)	67.75 (13.25)	29.00 (38.00) (months)
Gordon W. Duncan et al., 2015 [39]	HC	50 (29)	65.8 \pm 8.0	6.15 (4.66)
	PD	125 (85)	66.0 \pm 10.5	–
Abhishek Lenka et al., 2020 [40]	PD-NP	48 (41)	57.9 \pm 7.0	5.7 \pm 2.4
	PD-P	42 (35)	58.5 \pm 7.8	6.5 \pm 3.2
Rémi Patriat et al., 2022 [41]	HC	21 (10)	61.3 \pm 8.0	–
	PD–RSWA	20 (14)	63.0 \pm 8.6	2.1 \pm 1.5
	PD + RSWA	18 (9)	65.8 \pm 4.8	2.8 \pm 2.2
Yuanjing Feng et al., 2020 [42]	SWEDD	42 (27)	60.7 \pm 9.4	6.9 \pm 8.0
	PD	50 (35)	60.3 \pm 8.9	6.7 \pm 7.3
	HC	50 (35)	60.6 \pm 10.3	NA
Markus Nilsson et al., 2015 [43]	PDD	11 (NA)	74 \pm 7	NA
	HC	27 (NA)	70 \pm 4	–
Lubin Gou et al., 2018 [44]	d-PD	28 (17)	61.43 \pm 10.06	–
	nd-PD	56 (36)	63.97 \pm 8.31	NA
	HC	37 (21)	60.35 \pm 11.70	–

Table 1. Cont.

Demographic Features				
Study	Groups Studied	Number of Participants (Male)	Mean Age \pm SD (Years) or Range	Disease Duration \pm SD (Years) or Range
Rachel P. Guimarães et al., 2018 [45]	All PD	97	60.93 \pm 9.8	7.8 \pm 6.43
	MPD	24	61.66 \pm 9.6	4.15 \pm 4.08
	MoPD	60	60.30 \pm 10.69	8.74 \pm 6.62
	SPD	13	61.96 \pm 8.4	12.14 \pm 5.31
	HC	137 (83)	58 \pm 9.39	–
Chaoyang Jin et al., 2021 [46]	HC	24 (15)	62.5 \pm 3.8	–
	PD FOG +	24 (11)	65.5 \pm 6.1	6.00 \pm 5.25
	PD FOG–	37 (18)	64.1 \pm 8.2	3.01 \pm 3.21
Yunjun Yang et al., 2022 [47]	Dpd	37 (19)	60.73 \pm 11.22	5.01 \pm 3.01
	ndPD	35 (21)	62.40 \pm 11.10	3.57 \pm 3.65
	HC	25 (9)	57.08 \pm 7.93	–
Xiaojun Guan et al., 2018 [48]	HC	46 (21)	57.8 \pm 9.4	–
	PD	65 (32)	55.5 \pm 9.5	4.7 \pm 3.9
Elisa Canu et al., 2015 [49]	PD-FoG	23	66.9 \pm 8.0	\geq 5 years
	HC	35	67.7 \pm 7.6	–
Gong-Jun Ji et al., 2019 [50]	PD	57 (29)	59.5 1.21	4.6 0.61
	HC	52 (20)	60.6 1.22	–
Tao Guo et al., 2020 [51]	S-depression PD	53 (29)	60.89 \pm 8.68	3.86 \pm 4.14
	S-motor PD	37 (26)	63.34 \pm 10.05	4.86 \pm 3.03
	mild PD	44 (24)	59.38 \pm 8.30	3.77 \pm 3.58
	HC	77 (33)	60.22 \pm 7.40	–
Yiming Xiao et al., 2021 [52]	Left-dominant PD	62 (34)	59.8 \pm 8.8	NA
	Right-dominant PD	79 (56)	63.2 \pm 8.8	
	PD	141 (90)	61.7 \pm 8.9	
	HC	62 (22)	61.4 \pm 9.8	
Chih-Ying Lee et al., 2019 [53]	NC	19 (10)	60.3 7.6	–
	PDNSa	31 (9)	60.3 9.8	2.4 2.4
	PDSa	21 (12)	63.7 11.6	1.9 2.0
F Imperiale et al., 2017 [54]	PD-ICB	35 (30)	62.0 \pm 10.4	9.5 \pm 5.2
	PD no-ICB	50 (36)	61.5 \pm 8.9	9.0 \pm 6.1
	HC	50 (35)	59.0 \pm 12.4	NA
Hye Bin Yoo et al., 2015 [55]	PD-ICD	10 (7)	54.5 \pm 6.2	10.2 \pm 7.3
	PD-nonICD	9 (6)	59.6 \pm 8.6	10.6 \pm 3.9
	HC	18 (10)	54.4 \pm 6.5	–
Olaia Lucas-Jim'enez et al., 2015 [56]	PD	37 (22)	67.97 (6.17)	6.96 (5.61)
	HC	15 (11)	65.07 (7.01)	–
Takahiro Koinumaa 2021 [57]	HC	15 (9)	55.2 (\pm 20.7)	–
	PARK2	9 (4)	58.3 (\pm 14.1)	27.5 (\pm 11.9) months
Charalampos Georgiopoulos et al., 2017 [58]	PD	22 (12)	68 (95% CI 67 and 70)	7 (95% CI 5 and 9)
	HC	13	68 (95% CI 65 and 70)	–
Xiang-Rong Li et al., 2018 [59]	PD	31	60.5 \pm 9.3	NA
	HC	22	59.7 \pm 8.6	–
Kazufumi Kikuchi et al., 2017 [60]	PD-MIBGH	12	66.8 \pm 4.9	1 \pm 1.3
	PD-MIBGL	12	67.4 \pm 6.1	2 \pm 1.9
Virendra R. Mishra et al., 2019 [61]	HC	44 (29)	61 \pm 10.79	NA
	PD	81 (52)	61.35 \pm 9.93	11.46 \pm 13.85
Thais Minett et al., 2018 [62]	PD-NC	93	64.3 \pm 10.8	6.4 \pm 0.5
	PD-MCI	27	70.5 \pm 8.1	5.6 \pm 0.7
	HC	48	66.0 \pm 7.9	–
Maria Chondrogiorgi et al., 2019 [63]	PD-CTRL	40 (31)	68.4 (6)	5.7 (4.8)
	PDD	21 (16)	70.9 (5.7)	7.9 (6.8)
Yuko Koshimori et al., 2015 [64]	HC	26 (13)	70.5 \pm 5.6	6.7 (4.2)
	PD	15 (4)	67.13 \pm 5.1	–

Table 1. Cont.

Demographic Features				
Study	Groups Studied	Number of Participants (Male)	Mean Age \pm SD (Years) or Range	Disease Duration \pm SD (Years) or Range
Ming-fang Jiang et al., 2015 [65]	PD	31 (16)	69.4 \pm 8.0	< 3 years in 15 cases, 3–5 years in 9 cases, and 5–10 years in 7 cases
	HC	34 (18)	69.3 \pm 8.0	
Sara Pietracupa et al., 2017 [66]	PD-FOG	21 (16)	66.3 \pm 10.72	11 \pm 6.3
	PD-NFOG	16 (13)	69.7 \pm 11.1	9.5 \pm 6.2
	HC	19	66.74 \pm 7.68	-
A. Inguanzo et al., 2020 [67]	HC	33 (18)	66 (15)	NA
	PD1	15 (13)	75 (14)	7 (7.5)
	PD2	21 (14)	68 (9)	9 (9)
	PD3	26 (19)	58.5 (11)	7 (5.5)
Laura Pelizzari et al., 2019 [68]	LPD	9 (4)	68.3 (57.1–73.3)	4 (1.5–6)
	RPD	12 (7)	70.2 (61–73.8)	2 (1–3.5)
	HC	17 (9)	64.1 (57.3–68.3)	-
Tracy R. Melzer et al., 2015 [69]	HC	23 (16)	70.6 \pm 6.8	-
	PD	23 (17)	69.5 \pm 6.4	5.6 \pm 4.3
Yulia Surova 2016 [70]	HC	44 (19)	66 \pm 8	-
	PD	105 (44)	66 \pm 11	5 \pm 4
Takashi Ogawa 2021 [71]	HCS	23 (9)	67.0 \pm 1.2	-
	PD-nLID	26 (11)	67.2 \pm 4.7	7.3 \pm 3.9
	PD-LID	25 (10)	66.8 \pm 7.4	13.8 \pm 7.1
Jinqiu Yu et al., 2022 [72]	HC	28 (12)	62.3 \pm 6	NA
	PD	26 (14)	65.5 \pm 6.8	
	G/G	27 (14)	63.9 \pm 6.6	
	G/A	12 (12)	63.8 \pm 6.6	
Qin Shen et al., 2021 [73]	ndPD	30 (15)	56.9 \pm 10.6	2.2 \pm 1.2
	mdPD	22 (10)	56.4 \pm 8.0	2.3 \pm 1.3
	sdPD	15 (6)	57.8 \pm 6.7	2.5 \pm 1.5
Morinobu Seki et al., 2019 [74]	PSP	18 (14)	67.1 \pm 6.5	2.3 \pm 1.5
	MSA-P	16 (8)	63.9 \pm 7.1	1.9 \pm 1.6
	PD	16 (9)	65.2 \pm 5.3	3.2 \pm 2.0
	HC	21 (8)	62.3 \pm 6.8	-
Min Wang et al., 2016 [75]	PD-FOG	14 (9)	72.36 \pm 6.15	3.29 \pm 1.65
	PD-nFOG	16 (10)	68.88 \pm 6.00	3.70 \pm 2.94
	HC	16 (8)	68.56 \pm 2.56	-
Ming-Ching Wen et al., 2018 [76]	HC	61 (41)	60.19 \pm 10.80	7.52 \pm 8.00
	TD	52 (32)	60.46 \pm 9.57	6.54 \pm 6.78
	PIGD	13 (10)	66.66 \pm 10.17	-
Jingqiang Wang et al., 2020 [77]	PD	30 (19)	59.3 \pm 9.0	NA
	HC	28 (17)	59.9 \pm 9.7	
Yang Zhang et al., 2017 [78]	Apathy	18 (17)	62.28 \pm 13.02	4.06 \pm 2.34
	Non-apathy	21 (14)	60.24 \pm 10.32	3.74 \pm 2.50
Meng-Hsiang Chen et al., 2017 [79]	PD	29 (20)	61.51 \pm 8.27	NA
	HC	26 (19)	60.11 \pm 7.77	
Fuyong Chen et al., 2019 [80]	HC	20 (80%)	59.5 \pm 6.2	-
	PD-CN	19 (78.9%)	61.3 \pm 6.9	5.9 \pm 3.4
	PD-aMCI	17 (88.2%)	64.9 \pm 5.9	7.6 \pm 4.9
Elisa Canu et al., 2015 [49]	PD-punding	21 (18)	63.8 \pm 8.8	9.4 \pm 5.4
	PD no-ICB	28 (19)	63.6 \pm 6.5	9.7 \pm 5.4
	HC	28 (19)	61.9 \pm 8.3	-
Chin-Song Lu et al., 2016 [81]	PD	126 (68)	62.0 \pm 7.6	8.2 \pm 6.1
	HC	91 (43)	59.8 \pm 7.2	-
Wen Zhou et al., 2021 [82]	Responsive group	15 (7)	67.13 \pm 8.52	3.93 \pm 3.10
	Irresponsive group	11 (6)	68.91 \pm 7.08	2.82 \pm 2.75

Table 1. Cont.

Demographic Features				
Study	Groups Studied	Number of Participants (Male)	Mean Age \pm SD (Years) or Range	Disease Duration \pm SD (Years) or Range
Mina Ansari et al., 2016 [83]	PD-RBD	23 (18)	59.43 \pm 10.97	7.95 \pm 8.76 months
	PD-non-RBD	31 (20)	60.64 \pm 8.65	7.32 \pm 8.19 months
Suk Yun Kang et al., 2019 [84]	Without fatigue	23 (10)	70.0 \pm 8.4	22.7 \pm 28.5 months
	With fatigue	9 (8)	63.6 \pm 12.5	27.6 \pm 2.2 months
Lauren Uhr et al., 2022 [85]	PD	31 (24)	64.5 (5.80)	8.48 (3.38)
Jilu Princy Mole et al., 2016 [25]	PD	24 (20)	63.42 \pm 10.82	NA
	HC	26 (17)	64.88 \pm 8.06	

All studies except ten [36,40,53,60,63,73,82,84–86] included healthy controls.

The sample size of the PD patients varied widely, with a pilot study having only seven female participants [34] and the largest sample size being 205 from the prospective and longitudinal Swedish BioFINDER study [31].

The studies included both male and female participants, with most studies having a predominantly male population. One study [34] only included females, and two studies did not mention the gender distribution [43,45].

The disease duration of Parkinson's disease ranged from 1 \pm 1.3 years in one study [60] to 14.3 \pm 7.75 years in another study [35].

4. Cingulum

4.1. PD

A summary of the studies is presented in Table 2. PD is a progressive, degenerative disorder that affects multiple systems in the body. It is characterized by the accumulation of α -synuclein protein in various brain regions, leading to both motor and non-motor symptoms [31].

A previous study utilized DTI to demonstrate degeneration of the nigrostriatal pathway in PD patients. Results showed differences in FA and MD, highlighting the value of DTI in the diagnosis of PD [31].

A study conducted on animals examined the effectiveness of diffusion kurtosis imaging (DKI)—an extension of DTI—in detecting changes caused by the accumulation of α -synuclein (α -syn) in the white matter (specifically the cingulum) of α -syn over-expressing transgenic mice (TNWT-61). The findings suggest that DKI could serve as a highly sensitive method for identifying changes in brain tissue induced by α -synuclein accumulation, which may indicate the progression of Parkinson's disease [31].

The cingulum, being a vulnerable area in the brain, has drawn attention in neurodegenerative research. Research has suggested that evaluating the cingulum fibers through DTI could enhance early diagnosis of neurodegenerative diseases.

Decreased connectivity in the cingulum tract has been found to be negatively correlated with neutrophil-to-lymphocyte ratio (NLR) in the early stage of PD progression [31].

NLR is a non-invasive marker of peripheral neuroinflammation and increased NLR is associated with poor cellular immunity.

According to the results of the study, degeneration of central white matter tracts in the brain occurs early in Parkinson's disease and is primarily located in the cingulum. This degeneration may contribute to early cognitive dysfunction. Changes in the DTI measures, including increased MD [31,39,64,68] and decreased FA [50,59,65] have been detected in PD patients, with a higher number of group differences being found as the mean diffusivity increases.

Table 2. An overview of the literature regarding studies with significant microstructural changes of Cingulum in association with PD symptoms. (NA is a written abbreviation for not applicable.)

Study	Between-Group Findings			Additional imaging results	Symptomatology Correlations with DTI Metrics	Significant associations	Complementary Information of Participants	
	FA	MD	RD or AD increases		Applied tests		Drug exposure	Group matches
Zonghong Li et al., 2020 [27]	No significant differences	Non-depressed PD, depressed PD > HC in left uncinate fasciculus	RD: No significant differences AD: non-depressed PD, depressed PD > HC in right hippocampal part of cingulum and bilateral uncinate fasciculus	NA	HDRS, MMSE, UPDRS-III, H&Y	NA	NA	Age, sex, years of education or MMSE
Martin Gorges et al., 2019 [29]	PD < HC in cingulum	NA	NA	NA	H&Y, UPDRS-III, MMSE, PANDA, CERAD	Significant correlations between cognitive state-dependent regional FA changes and the sociodemographically corrected CERAD total score in cingulum	ON	
Mattis Jalakas et al., 2019 [31]	NA	NA	NA	NA	UPDRS-III, MMSE	Correlations between declining processing speed and discrepancies in the cingulum tract using the mean diffusivity, MD, parameter	ON	
Christina Andica et al., 2019 [32]	HC > PD in UF and cingulum hippocampus	HC < PD in UF	AD: HC < PD in UF RD: HC < PD in UF and cingulum hippocampus	NA	MDS-UPDRS, H&Y	NA	ON	
Christina Andica et al., 2020 [33]	HC > PD-woNCP in UF and right cingulum hippocampus HC > PD-wNCP in cingulum hippocampus and UF	HC < PD-woNCP in UF HC < PD-wNCPs in right cingulum hippocampus and UF	RD: HC < PD-woNCP in UF and cingulum hippocampus HC < PD-wNCP in UF and cingulum hippocampus AD: HC < PD-wNCP in UF	TOI: FA: PD-woNCP < HC PD-wNCP < HC MD: PD-woNCP > HC PD-wNCP > HC RD: PD-woNCP > HC PD-wNCP > HC	H&Y, UPDRS I, UPDRS-III, TOI	NA	ON	Age and sex-matched HCs
Nan-Kuei Chen et al., 2018 [34]	PD > HC in Cingulum (hippocampus)	NA	NA	NA	MMSE, UPDRS-III, H&Y	The FA values negatively correlated with the UPDRS-III scores across PD patients in Cingulum (hippocampus) and UF	NA	

Table 2. Cont.

	Between-Group Findings		Symptomatology Correlations with DTI Metrics			Complementary Information of Participants		
Haruka Takeshige-Amano et al., 2022 [35]	NA	PD-ICB > HC in uncinate fasciculus PD-nICB > PD-ICB in cingulum and UF	NA	NA	H&Y, UPDRS I, UPDRS-III	NA	ON	
Jia-Yong Wu et al., 2017 [36]	PDD < PDnD in UF and cingulum	NA	NA	NA	UPDRS-III, H&Y, MMSE, HDRS	FA values in the left cingulum and left superior longitudinal fasciculus of the PDD group were negatively correlated with HDRS scores, but no correlation was found with other disease characteristics including age, duration, UPDRS-III, H-Y scale, MMSE	NA	Age, age of onset, disease duration, sex
Jingwen Chen et al., 2022 [37]	LAR, LTD < HC No significant differences between RAR, RTD and HC in cingulum bundle	No significant differences	NA	NA	UPDRS-III, H&Y, MMSE	NA	ON	Age, disease duration, sex, Levodopa equivalent daily dos
Gordon W. Duncan et al., 2015 [39]	No significant difference	PD > HC in cingulum	NA	NA	MDS-UPDRS-III, H&Y, MMSE, MoCA	NA	ON	Age, gender, and education
Abhishek Lenka et al., 2020 [40]	PD-P < PD-NP in cingulum	No significant difference	No significant difference	NA	MoCA, HAMD, HAMA, H&Y, FAB, UPDRS-III, Corsi block-tapping test, RAVLT, CFT, TMT-B, Stroop effect	NA	ON	Age, sex, age of onset, disease duration
Rémi Patriat et al., 2022 [41]	NA	PD-RSWA < HC in cingulum	RD: PD-RSWA < HC in cingulum	NA	MDS-UPDRS-III, H&Y, MoCA	NA	ON	Sex, age, education and MoCA, age at diagnosis, years since diagnosis, H&Y AND total MDS UDRS III score
Yuanjing Feng et al., 2020 [42]	SWEDD < PD, HC PD > HC in cingulum bundle	NA	AD: SWEDD > PD, HC in cingulum bundle	NA	UPDRS-III, MoCA	NA	NA	
Markus Nilsson et al., 2015 [43]	PDD > HC in cingulum	NA	NA	NA	NA	NA	NA	

Table 2. Cont.

	Between-Group Findings				Symptomatology Correlations with DTI Metrics		Complementary Information of Participants	
Rachel P. Guimarães et al., 2018 [45]	All PD < HC in cingulum	NA	RD: ALL PD > HC in cingulum SPD > HC, MPD, MoPD in cingulum	ROI: no FA difference between groups. AD and RD were higher in SPD when compared to HC, MPD and MoPD	UPDRS, UPDRS-PartIII, H&Y, SCOPA, SCOPA, NMSS	Positive association between SCOPA-COG scores and FA values, and a negative association with RD and UPDRS, UPDRS-III and NMSS, were positively associated with AD and RD values in cingulum	ON	Age and sex
Chaoyang Jin et al., 2021 [46]	PD FOG+ < HC PD FOG+ < PD FOG− in the cingulum	PD FOG− > HC in cingulum	NA	NA	UPDRS-III, H&Y, FOGQ, MMSE, MoCA, TUG, HDRS NA, HARS	NA	NA	
Yunjun Yang et al., 2022 [47]	dPD < ndPD in right cingulum (cingulate gyrus), left cingulum hippocampus	dPD > ndPD in right cingulum (cingulate gyrus)	NA	NA	H&Y, UPDRS- III, HAM-D, HAMA, MMSE, MoCA	NA	NA	
Xiaojun Guan et al., 2018 [48]	PD < HC only in the right UF	PD > HC in the left cingulum	RD: PD > HC AD: PD < HC	NA	UPDRS, H&Y, MMSE	In the right cingulate gyrus, significant correlation of increased MMS with disease duration	NA	Age and sex
Elisa Canu et al., 2015 [49]	PD-FoG < HC in cingulum	PD-FoG > HC in cingulum	NA	NA	FOGQ, UPDRS-III	NA	ON	Age, sex, education
Gong-Jun Ji et al., 2019 [50]	PD < HC in the left cingulum	NA	NA	NA	UPDRS-III, H&Y, MMSE, MoCA	No significant correlation was found between FA in the left cingulum and clinical measures	51 of PD patients OFF, 6 ON	Age, sex, and education-matched HCs
Yiming Xiao et al., 2021 [52]	PD > HC in cingulum Right dominant PD > Left dominant PD in cingulum	NA	NA	NA	H&Y, UPDRS, GDS, RBDSQ	NA	NA	
Chih-Ying Lee et al., 2019 [53]	PDSa < PDNsa in bilateral cingulum	PDSa > PDNsa in bilateral cingulum	RD: PDSa > PDNsa in bilateral cingulum	NA	UPDRS, H&Y, MMSE, S&E, ASMI	Significantly associations between ASMI and FA of the ROI in the left cingulum	ON	Age, gender, height, MMSE
Hye Bin Yoo et al., 2015 [55]	PD-ICD > PD-nonICD in right dorsal and posterior cingula	NA	NA	NA	MMSE, UDPRS, H&Y	NA	ON	Age, sex, MMSE score, GDS score, disease duration, total daily LED, UPDRS, HY stage

Table 2. Cont.

	Between-Group Findings			Symptomatology Correlations with DTI Metrics			Complementary Information of Participants	
Olaia Lucas-Jimenez et al., 2015 [56]	PD < HC in right ACT PD > HC in left PCT	NA	NA	NA	UDPRS, H&Y	In correlations between verbal memory and FA of the right PCT, FA correlated positively with correct rejections and negatively with false positives in HC group between brain activation in the left IOFC during the verbal learning memory fMRI task and FA of the right UF	ON	
Xiang-Rong Li et al., 2018 [59]	PD < HC in left unciform fasciculus, right cingulum	NA	NA	NA	H&Y, UPDRS, MMSE	UPDRS and motor score had no relationship with the FA of each white matter fasciculus	OFF	
Virendra R. Mishra et al., 2019 [61]	No significant differences	No significant differences	No significant differences	NA	MDS-UPDRS-III, MoCA, H&Y	TBSS: Negative correlation with disease duration and bilateral CGC DTI-TK: Positive correlation with disease duration and RD in left CGC	NA	Sex, age, years of education, and handedness and MoCA
Thais Minett et al., 2018 [62]	PDMCI < HC in cingula	PD-MCI and PD-N > HC in cingula	NA	NA	UPDRS-III, H&Y	NA	ON	Age, proportion of WML, duration of PD, levodopa equivalent dose
Maria Chondrogiorgi et al., 2019 [63]	PDD < PD-CTRL in cingulum (cingulate gyrus) and uncinate fasciculus	No significant differences	No significant differences	NA	H&Y, MMSE, HAM-D, PD-CRS	Lower total PD-CRS score was associated with FA decreases in cingulum (cingulate gyrus), cingulum (hippocampus) and uncinate fasciculus	ON	Sex, years of education
Yuko Koshimori et al., 2015 [64]	NA	PD > HC in cingulum and uncinate fasciculus	NA	NA	MoCA, UPDRS-III,	NA	ON	Age, sex, education, BDI, and handedness
Ming-fang Jiang et al., 2015 [65]	PD < HC in cingulum bundle	NA	NA	NA	H&Y, UPDRS-III, MoCA, ADL, HAMD	FA values in the white matter tracts showed no correlation with UPDRSIII scores	ON	Age and sex

Table 2. Cont.

Between-Group Findings		Symptomatology Correlations with DTI Metrics			Complementary Information of Participants			
Sara Pietracupa et al., 2017 [66]	NA	HC < PD-FOG, PD-NFOG PD-FOG > PD-NFOG in UF HC, PD-FOG < PD-NFOG HC < PD-FOG in Cingulum angular bundle	RD: HC < PD-FOG, PD-NFOG PD-FOG < PD-NFOG in UF HC, PD-FOG < PD-NFOG HC < PD-FOG in Cingulum angular bundle AD: HC, PD-FOG < PD-NFOG HC > PD-FOG in UF	NA	H&Y, UPDRS-III, MMSE, FAB, HAM-D	DTI values in the uncinate fasciculus and cingulum (both cingulate gyrus and angular bundles) bilaterally significantly correlated with the cognitive scores, as assessed by the MMSE DTI values in the uncinate fasciculus and cingulum (angular bundle and cingulate gyrus) bilaterally significantly correlated with frontal abilities, as indicated by the FAB scores significant correlation between DTI values in the right uncinate fasciculus and the HAM-D scores	ON & OFF	Age and sex
Laura Pelizzari et al., 2019 [68]	No significant differences	RPD > HC in right cingulum LPD > HC RPD > LPD	No significant differences	NA	MDS-UPDRS-III, H&Y, MoCA	NA	ON	
Tracy R. Melzer et al., 2015 [69]	No significant differences	No significant differences	No significant differences	Time effects: FA showed widespread reduction in cingulum bundles, MD, and RD exhibited significant, yet more restricted increases	MDS-UPDRS-III	NA	ON	Age, education, sex
Yulia Surova 2016 [70]	PD > HC in Cingulum hippocampus	NA	NA	NA	UPDRS, H&Y, MMSE, AQT, ADAS-Cog	NA	NA	
Morinobu Seki et al., 2019 [74]	NA	PD, HC > MSA-P in adjacent cingulum	NA	NA	UPDRS-III, H&Y, MMSE	NA	NA	Sex, age, and disease duration
Min Wang et al., 2016 [75]	PD-FOG < HC in left cingulum	PD-FOG > HC in left cingulum	NA	NA	FOGQ, MMSE, UPDRS-III	NA	ON	Age, sex, education PD-FOG and PDnFOG: Disease duration, UPDRS-III, LEDD

Table 2. Cont.

	Between-Group Findings				Symptomatology Correlations with DTI Metrics		Complementary Information of Participants
Ming-Ching Wen et al., 2018 [76]	TD > HC in right cingulum TD > PIGD in right and left cingulum no significant between HC and PIGD	NA	RD: TD < HC in right cingulum, PIGD > TD in UF AD: PIGD > HC in UF	NA	UDPRS, H&Y, MOCA, GDS, Cardiovascular burden, Head motion	NA	OFF Age, sex, education, handedness, dominant side, PD duration/H&Y scale, cardiovascular burden, head motion
Jingqiang Wang et al., 2020 [77]	Significant Difference in UF	NA	AD: Significant Difference in cingulum bundle		MoCA, UPDRS-III, GDS	Cingulum bundle have correlation with GDS	NA
Yang Zhang et al., 2017 [78]	apathy group < Non-apathy in left cingulum	NA	NA	NA	H&Y, UPDRS-III, MMSE, BDI-II	FA and LARS scores were negatively correlated in left cingulum	ON Age, sex, disease duration, LEDD, UPDRS-III, MMSE
Meng-Hsiang Chen et al., 2017 [79]	PD < HC in left cingulum	NA	NA	NA	H&Y, UPDRS-III, S&E	MD values in the left cingulum were positively correlated with baroreflex sensitivity and negatively correlated with serum nuclear DNA simultaneously AD values in the left cingulum were positively correlated with the serum nuclear DNA level RD values in the left cingulum were simultaneously positively correlated with baroreflex sensitivity and negatively correlated with serum nuclear DNA	NA Age and sex
Fuyong Chen et al., 2019 [80]	PD-CN > PD-aMCI in cingulum (cingulate gyrus) in the bilateral hemispheres	NA	NA	NA	H&Y, UPDRS-III, MMSE, RBANS	NA	ON
Chin-Song Lu et al., 2016 [81]	NA	NA	NA	NA	H&Y, UPDRS-III, MMSE, ADL	A statistically significant association between ADL and maximum MD/RD in the ipsilateral posterior cingulum	OFF

Table 2. Cont.

	Between-Group Findings				Symptomatology Correlations with DTI Metrics		Complementary Information of Participants	
Wen Zhou et al., 2021 [82]	Irresponsive group < Responsive group in bilateral cingulum	NA	NA	NA	H&Y, UPDRS-III, MMSE	NA	ON	Parkinson's disease duration, age, sex
Mina Ansari et al., 2016 [83]	PD-RBD < PD-non-RBD in cingulum	NA	NA	NA	RBD, MOCA, GDS, UPDRS-III, H&Y, ESS, LNS	NA	NA	Age, sex
Suk Yun Kang et al., 2019 [84]	PD < PD with fatigue in right cingulum, UF	PD > PD with fatigue in right cingulum	RD: PD > PD with fatigue in UF, cingulum	NA	K-MMSE, MoCA, BDI, UPDRS, H&Y, FSS	NA	NA	
Lauren Uhr et al., 2022 [85]	NA	NA	NA	NA	UPDRS	Positive ROI-based correlations of FA and depressive symptoms in left cingulum (hippocampus)	ON	

Studies have suggested that MD may be more sensitive in detecting subtle white matter changes in early PD than FA, as has been found in other studies in early Alzheimer patients [87].

The pattern of decreased FA and increased MD and RD is indicative of neurodegeneration [48], which has been found in individual PD patients in the present study [33].

Three studies [34,52,70] suggest that the cingulum (where the FA of PD patients is greater than the FA of controls) is modulated by PD through a compensatory mechanism. The FA measures obtained from these brain regions may potentially be used to detect brain signal changes in an early stage of PD, possibly even before the clinical manifestation of motor symptoms [34].

The exact cause of the changes observed in the DTI of PD patients remains unknown, but it is believed to be due to variations in the diffusion ellipsoid dimensions caused by the neurodegenerative process. While FA is commonly used as a measure of white matter integrity, this interpretation should be approached with caution as it is influenced by various factors such as myelination, axon packing, membrane permeability, internal axonal structure, and tissue water content [88].

The findings of some studies have shown decreased FA and increased RD [45] in the cingulum of PD patients, while others have found increased FA and decreased AD in the same region [42]. It is hypothesized that extensive damage to white matter fibers occurs in the early stages of PD, potentially due to the aggregation of synapsins and Lewy bodies in vulnerable brain regions, resulting in atrophy, neuron loss, and demyelination of nerve fibers [89].

4.2. Motor Symptoms

In comparison to healthy controls (HC), most studies found degeneration in PD patients with motor symptoms, as indicated by decreased FA [37,79,83], increased MD [74] and a combination of decreased FA and increased MD [46]. These results suggest that FA, MD, and other DTI measures could serve as quantitative biomarkers of motor symptom severity in PD. Lower FA is typically associated with decreased WM connectivity and is considered an indication of WM microstructural abnormalities. However, it is unclear why these changes occur. Motor symptoms usually appear late in PD patients, which suggests that decreases in FA occur later in the disease than increases in MD. Some studies have found increased FA in PD patients [52,60].

The cingulum, an association fiber that connects anterior and posterior cortical regions, showed increased FA or decreased MD/RD in PD patients and was associated with better olfaction and lower motor severity [76,90].

These findings suggest that increased connectivity in these WM structures could serve as a compensatory mechanism to facilitate efficient information transfer between different regions of the brain.

4.3. Non-Motor Symptoms

It has been found in most studies that individuals with PD who have non-motor symptoms such as dementia, depression, cognitive impairment, psychosis, or apathy have significantly decreased FA values compared to HC [29,36,40,56,80,86].

The pattern of decreased FA and increased mean diffusivity (MD) has also been shown in several studies [33,47,62].

In some studies, compensation was also defined by increased FA or decreased MD [43,55,84].

Studies have consistently shown that an increase in MD (AD and RD) is associated with cell atrophy and demyelination, which may indicate extensive degeneration in advanced PD patients who present with dominant non-motor symptoms. This loss of structural organization is believed to be linked to neurodegeneration.

Depression and dementia frequently occur in PD patients, often appearing late in the disease at stage 3 or 4 of the Hoehn and Yahr staging for motor involvement. They can also be present early on in the honeymoon period of PD, and have been shown to correlate with

the severity of motor involvement [37]. Abnormal functioning in depression and dementia in PD patients may be due to degeneration of the microstructure in the white matter located in frontal-limbic regions. This has been observed in previous studies, and one hypothesis is that abnormalities in the frontal limbic system cause depression in PD patients [27].

Disruption of the structural integrity of white matter in the cingulum tract can be recognized as a marker to predict early PD, regardless of white matter alteration related to REM sleep disorder [83,91], depression [91,92], or olfaction dysfunction [93], which are thought to be early nonmotor symptoms of PD.

Thus, changes in the cingulum microstructure could be used to detect early stages of PD and help distinguish between PD patients without dementia and depression or those in preclinical stages.

4.4. Correlation

DTI values in the cingulum have been shown to be significantly associated with cognitive function in PD patients. This was demonstrated by a correlation between DTI values and scores from the Mini-Mental State Examination (MMSE) and the Frontal Assessment Battery (FAB). The study results indicate that the more extensive the diffusivity abnormalities in the cingulum, the worse the cognitive performance [66].

Spearman rank order correlation analyses found significant correlations between changes in FA values in the cingulum and sociodemographically corrected Consortium to Establish a Registry for Alzheimer's Disease (CERAD) total scores in PD patients [29].

Additionally, lower scores on the Parkinson's Disease-Cognitive Rating Scale (PD-CRS) were associated with decreases in FA values in the cingulum [63]. A novel finding from one study showed a linear association between AD and the PD-CRS score in major WM tracts, without concurrent RD alterations. This suggests that extensive and progressive axonal degeneration, without evident demyelination, may be involved in cognitive impairment in PD [94,95].

The cingulum bundle has a correlation with the short Geriatric Depression Scale (GDS) [42].

In one study, the FA values in the left cingulum of PD patients with depression were negatively correlated with the Hamilton Depression Rating Scale (HDRS) scores, but no correlation was found with other disease characteristics such as age, duration, Unified Parkinson Disease Rating Scale III (UPDRS III), H&Y scale, and MMSE [36]. Another study found that the FA values negatively correlated with the UPDRS-III scores across all PD patients in the cingulum [34]. Positive correlation with disease duration and RD in the left cingulum was revealed by using Tensor-based registration (DTI-TK) and negative correlation by TBSS. The study suggested a preference for the DTI-TK based registration technique before statistical analysis [61].

On the other hand, some studies found no significant correlation between FA in the left cingulum and clinical measures [50,73].

A significant association was also found between FA of the ROI in the left cingulum and appendicular skeletal muscle mass index (ASMI). Low FA values in the left cingulum were identified as the strongest predictor of sarcopenia in PD patients [53]. Positive correlations of FA and non-motor symptoms such as depressive symptoms were also found in the left cingulum in some studies [85].

Interestingly, it has been found that PD risk can be affected by cardiovascular risk factors including serum cholesterol and apo-lipoprotein levels [96].

In the early stages of PD, apo-lipoprotein A1 might predict the microstructural changes of certain white matter tracts like the cingulum [97].

The relationships between clinical presentations, MD, AD, RD, and serum nuclear DNA levels have also been demonstrated. Results suggest that poor cardiovascular autonomic status in PD patients not only directly affects the white matter microstructure but also increases the serum nuclear DNA level, further impacting the white matter microstructure [79].

Impairment of the ipsilateral posterior cingulum in PD may reflect the loss of dopaminergic inputs from the midbrain, as indicated by the statistically significant association between Activities of Daily Living (ADL) and maximum MD/RD [81].

A correlation between verbal memory and FA in the right posterior cingulum tract (PCT) was found, with greater FA in the right PCT being associated with better performance in verbal recognition memory, a core process in subsequent recognition memory [56].

The Lille Apathy Rating Scale (LARS) scores of the apathetic PD group were negatively correlated with the FA values in the left cingulum [86].

The AD and RD values were positively associated with the UPDRS, UPDRS-III, and NMSS scores in the cingulum [45].

A negative association between RD and a positive association between FA values and the Scales for Outcomes in Parkinson's disease—Cognition (SCOPA-COG) scores were found in the cingulum [45].

One study found correlations between the MD parameter and declining processing speed and discrepancies in the cingulum tract [31].

5. Uncinate Fasciculus

5.1. PD

A summary of the included studies is presented in Table 3. The uncinate fasciculus interacts with the orbitofrontal cortex, assigning value to stored representations through interactions with temporal lobe-based information related to reward and punishment [98].

The most common cause of PD in autosomal recessive families is mutations in the parkin gene (PRKN) [99].

Tract-based spatial statistics (TBSS) using permutation analysis of linear models (PALM) has revealed elevated radial diffusivity (RD) in patients with parkin dysfunction (PRKN) compared to HCs. This finding is considered to be one of the most prominent pathological manifestations of parkin dysfunction, as it has been demonstrated by the elevated RD in multiple tests [57]. Another study [72] also confirms these results and suggests that PRKN patients with widespread increases in RD are more susceptible to widespread demyelination.

Different methods, including convolutional neural network (CNN) based methods, have shown that patients with PD exhibit increased mean diffusivity (MD) values [35,38,49,51,64]. However, some studies have reported decreased fractional anisotropy (FA) values [44,48,59,67]. MD appears to be more sensitive at detecting subtle changes in white matter in the early stages of PD compared to FA. It is due to damages to axons and neurons, as well as loss of myelin integrity in PD, that might result in decreased restriction of water molecule displacement, leading to higher MD values in PD patients [100].

A distinct pattern of neurodegeneration, characterized by low FA, high MD, low AD, and high RD, has been identified in PD patients [48]. This pattern was observed in a study by Andica et al. using TBSS [32] suggesting that PD patients are more susceptible to degeneration of the uncinate fasciculus (UF).

Christina Andica et al. conducted an analysis of white matter (WM) and gray matter in PD patients using TBSS. They found that PD patients with neurocognitive and psychiatric disorders (PD-wNCP) and PD patients without these disorders (PD-woNCP), compared to healthy controls (HCs), exhibited lower fractional anisotropy (FA), higher mean diffusivity (MD), higher radial diffusivity (RD), and higher axial diffusivity (AD), which has been described as neurodegeneration [33]. This pattern has previously been defined as neurodemyelination [48].

Table 3. An overview of the literature regarding studies with significant microstructural changes in the uncinate fasciculus in association with PD symptoms. (NA is a written abbreviation for not applicable.)

Study	Between-Group Findings			Additional imaging results	Symptomatology Correlations with DTI Metrics	Complementary Information of Participants		
	FA	MD	RD or AD increases		Applied tests	Significant associations	Drug exposure	Group matches
Boyu Chen et al., 2015 [26]	PD-Cu > PDD in bilateral uncinate fasciculus	PDD > PD-Cu in bilateral uncinate fasciculus HC > PDD	NA	NA	UPDRS-III, H&Y, MoCA, MMSE	MD value is negatively correlated with MoCa scores in UF	NA	
Zonghong Li et al., 2020 [27]	No significant differences	Non-depressed PD, depressed PD > HC in left uncinate fasciculus	RD: No significant differences AD: non-depressed PD, depressed PD > HC in right hippocampal part of cingulum and bilateral uncinate fasciculus	NA	HDRS, MMSE, UPDRS-III, H&Y	NA	NA	Age, sex, years of education or MMSE
Florian Holtbernd et al., 2019 [28]	PD, RBD > HC in left uncinate fasciculus	No significant difference between RBD, PD, and HC	No significant difference between RBD, PD, and HC	NA	MDS UPDRS-III, MoCA, H&Y	NA	ON	Age-matched HCs
Junyan Sun et al., 2021 [30]	NA	PD > HC in bilateral uncinate fasciculus	NA	NA	H&Y, UPDRS-III	NA	NA	Age, sex, education-matched HCs
Christina Andica et al., 2019 [32]	HC > PD in UF and cingulum hippocampus	HC < PD in UF	AD: HC < PD in UFRD: HC < PD in UF and cingulum hippocampus	NA	MDS-UPDRS, H&Y	NA	ON	
Christina Andica et al., 2020 [33]	HC > PD-woNCP in UF and right cingulum hippocampus HC > PD-wNCP in cingulum hippocampus and UF	HC < PD-woNCP in UF HC < PD-wNCPs in right cingulum hippocampus and UF	RD: HC < PD-woNCP in UF and cingulum hippocampus HC < PD-wNCP in UF and cingulum hippocampus AD: HC < PD-wNCP in UF	TOI: FA: PD-woNCP < HCPD-wNCP < HC MD: PD-woNCP > HCPD-wNCP > HCRD: PD-woNCP > HCPD-wNCP > HC	H&Y, UPDRS I, UPDRS-III, TOI	NA	ON	Age and sex-matched HCs
Nan-Kuei Chen et al., 2018 [34]	PD > HC in Cingulum (hippocampus)	NA	NA	NA	MMSE, UPDRS-III, H&Y	The FA values negatively correlated with the UPDRS-III scores across PD patients in Cingulum (hippocampus) and UF	NA	
Haruka Takeshige-Amano et al., 2022 [35]	NA	PD-ICB > HC in uncinate fasciculus PD-nICB > PD-ICB in cingulum and UF	NA	NA	H&Y, UPDRS I, UPDRS-III	NA	ON	

Table 3. Cont.

	Between-Group Findings				Symptomatology Correlations with DTI Metrics		Complementary Information of Participants	
Jia-Yong Wu et al., 2017 [36]	PDD < PDnD in UF and cingulum	NA	NA	NA	UPDRS-III, H&Y, MMSE, HDRS	FA values in the left cingulum and left superior longitudinal fasciculus of the PDD group were negatively correlated with HDRS scores, but no correlation was found with other disease characteristics including age, duration, UPDRS-III, H-Y scale, MMSE	NA	Age, age of onset, disease duration, sex
Sonia Di Tella et al., 2020 [38]	No significant differences	PD > HC in left UF	NA	NA	H&Y, UPDRS-III	FA of the left UF was positively correlated with the accuracy in the global word production (N + V), N production, V production and semantic fluency. FA of the right UF was positively correlated with the global word production and N production. No significant correlations were observed between FA and MD and the three measures of production task (N, V and N + V production)	ON	Age, sex, disease duration and years of education
Lubin Gou et al., 2018 [44]	All PD < HC in left uncinat fasciculus	NA	NA	NA	MoCA, MDS-UPDRS-III, H&Y	NA	OFF	Sex, age, MoCA, and education years
Xiaojun Guan et al., 2018 [48]	PD < HC only in the right UF	PD > HC in the left cingulum	RD: PD > HC AD: PD < HC	NA	UPDRS, H&Y, MMSE	In the right cingulate gyrus, significant correlation of increased MMS with disease duration	NA	Age and sex
Tao Guo et al., 2020 [51]	No significant differences in the FA	S-depression > HC in uncinat fasciculus No difference in the MD among the other pairs of comparisons	NA	NA	GCO, PDQ-39, UPDRS, H&Y, MMSE	NA	ON	Age, sex, education
F Imperiale et al., 2017 [54]	PD-ICB < PD no-ICB, HC in left uncinat fasciculus	PD-ICB > PD no-ICB, HC in right uncinat fasciculus	NA	NA	QUIP, H&Y, UPDRS-III, HDRS	NA	ON	All matched in: Age, sex, Education Patients matched in age at PD onset disease duration Side of onset H&Y scores UPDRS-III cognitive status

Table 3. Cont.

	Between-Group Findings				Symptomatology Correlations with DTI Metrics	Complementary Information of Participants	
Olaia Lucas-Jimenez et al., 2015 [56]	PD < HC in right ACTPD > HC in left PCT	NA	NA	NA	UDPRS, H&Y	In correlations between verbal memory and FA of the right PCT, FA correlated positively with correct rejections and negatively with false positives in HC group between brain activation in the left IOFC during the verbal learning memory fMRI task and FA of the right UF	ON
Takahiro Koinumaa 2021 [57]	HC < PARK2 in uncinate fasciculus	RD: HC < PARK2 in uncinate fasciculus	NA	NA	UDPRS III, H&Y	In PRKN AD values were negatively correlated with the serum levels of 9-hydroxystearate, while the MD and RD values were positively correlated with these levels in UF	ON Sex, age, cerebrovascular risk factors
Charalampos Georgiopoulos et al., 2017 [58]	NA	NA	AD: PD < HC in left uncinate fasciculus	NA	UPDRS-III, H&Y, MMSE	NA	ON Age, sex
Kazufumi Kikuchi et al., 2017 [60]	PD-MIBGL < PD-MIBGH in left uncinate fasciculus	No significant differences	NA	NA	MDS, H&Y, MMSE	NA	ON Age, sex, disease duration, MMSE, H&Y stage
Maria Chondrogiorgi et al., 2019 [63]	PDD < PD-CTRL in cingulum (cingulate gyrus) and uncinate fasciculus	No significant differences	No significant differences	NA	H&Y, MMSE, HAM-D, PD-CRS	Lower total PD-CRS score was associated with FA decreases in cingulum (cingulate gyrus), cingulum (hippocampus) and uncinate fasciculus	ON Sex, years of education
Yuko Koshimori et al., 2015 [64]	NA	PD > HC in cingulum and uncinate fasciculus	NA	NA	MoCA, UPDRS-III,	NA	ON Age, sex, education, BDI and handedness

Table 3. Cont.

Between-Group Findings			Symptomatology Correlations with DTI Metrics			Complementary Information of Participants		
Sara Pietracupa et al., 2017 [66]	NA	HC < PD-FOG, PD-NFOGPD-FOG > PD-NFOGin UFHC, PD-FOG < PD-NFOGHC < PD-FOG in Cingulum angular bundle	RD: HC < PD-FOG, PD-NFOGPD-FOG < PD-NFOGin UFHC, PD-FOG < PD-NFOGHC < PD-FOG in Cingulum angular bundleAD: HC, PD-FOG < PD-NFOGHC > PD-FOG in UF	NA	H&Y, UPDRS-III, MMSE, FAB, HAM-D	DTI values in the uncinat fasciculus and cingulum(both cingulate gyrus and angular bundles) bilaterallysignificantly correlated with the cognitive scores, as assessedby the MMSEDTI values in the uncinat fasciculus and cingulum(angular bundle and cingulate gyrus)bilaterally significantly correlated with frontal abilities, asindicated by the FAB scoressignificant correlation between DTI values in the right uncinat fasciculus and the HAM-D scores	ON and OFF	Age and sex
A. Inguanzo et al., 2020 [67]	PD1 < HC inuncinate fasciculus	NA	NA	NA	UPDRS-III, H&Y, MMSE	NA	ON	Sex andyears of education
Takashi Ogawa 2021 [71]	PD-nLID < HCPD-nLID < PD-LID in uf	NA	NA	NA	MDS-UPDRS, H&Y	NA	ON	Age, sex
Jinqiu Yu et al., 2022 [72]	G/G > G/A in UF	NA	RD: G/G < G/A in UF	NA	MMSE, MoCA, H&Y, UPDRS-III	NA	ON	
Qin Shen et al., 2021 [73]	sdPD < ndPD in UFsdPD < mdPD in UFNo significant difference between ndPD and mdPD	NA	RD: sdPD > ndPD in UF	NA	H&Y, MMSE, CDR, UPDRS-III, BDI	Nosignificant correlation was found between BDI scores andFA values in other tracts.	NA	Age, sex, education, CDR, MMSE, PD duration, H&Y scales, and UPDRS-III scores
Ming-Ching Wen et al., 2018 [76]	TD > HC in right cingulumTD > PIGD in right and left cingulumno significant between HC and PIGD	NA	RD: TD < HC in right cingulum, PIGD > TD in UFAD: PIGD > HC in UF	NA	UDPRS, H&Y, MOCA, GDS, Cardiovascular burden, Head motion	NA	OFF	Age, sex, education, handedness, dominant side, PDduration/H&Y scale, cardiovascular burden, head motion
Jingqiang Wang et al., 2020 [77]	SignificantDifference in UF	NA	AD: SignificantDifference in cingulum bundle		MoCA, UPDRS-III, GDS	Cingulum bundle have correlation with GDS	NA	

Table 3. Cont.

	Between-Group Findings				Symptomatology Correlations with DTI Metrics	Complementary Information of Participants		
Elisa Canu et al., 2015 [49]	NA	PD-punding > HC in right uncinate fasciculus	NA	NA	H&Y, UPDRS-III, MMSE, HAMA, HDRS	NA	ON	Age, sex, and education
Suk Yun Kang et al., 2019 [84]	PD < PD with fatigue in right cingulum, UF	PD > PD with fatigue in right cingulum	RD: PD > PD with fatigue in UF, cingulum	NA	K-MMSE, MoCA, BDI, UPDRS, H&Y, FSS	NA	NA	
Jilu Princy Mole et al., 2016 [25]	PD < HC in UF	PD > HC in left UF	RD: PD > HC in right UF	NA	UDPRS, H&Y, MOCA	NA	ON	

5.2. Motor Symptoms

The exact role of the UF in the development of motor symptoms in Parkinson's disease is still not clear. Only a few studies have investigated the effect of the uncinat fasciculus on motor symptoms, with inconsistent results [28,66,71].

5.3. Non-Motor Symptoms

Parkinson's disease, along with other neurodegenerative diseases such as Alzheimer's disease, frontotemporal dementia, and apathy, is characterized by non-motor symptoms that are associated with white matter (WM) pathways, including the UF and cingulum [101].

Changes in diffusion tensor imaging (DTI) measures have been observed in the UF in PD patients with cognitive impairment, depression, and apathy. This suggests that non-motor symptoms in PD are related to the impairment of long white matter nerve fibers. It is known that multiple neurotransmitter pathways, including noradrenergic and cholinergic pathways, that project to the frontal lobe are impaired in PD patients with non-motor symptoms and other non-cognitive problems [102–106].

Studies have reported that patients with non-motor symptoms such as depression, dementia, and cognitive impairment exhibit more degeneration, as indicated by decreased FA [36,63,80], increased MD [26,73], and increased mean diffusivity and AD [27].

A significant reduction in white matter connectivity in UF has been found in PD patients with depressive symptoms compared to non-depressed patients. The pathophysiology of depression has been extensively studied in relation to UF, with reduced FA serving as a marker for tract microstructural alteration in individuals with major depressive disorder (MDD) [107]. Although Delaparte et al. [108] could not identify any significant differences between anxious and non-anxious depression, anxiety, which is frequently associated with depression, has been demonstrated to be connected to disrupted UF [108,109].

Previous research [23,110,111] has defined degeneration in the UF as low FA and high MD in patients with impulsive–compulsive behaviors and PD with neurocognitive and psychiatric symptoms [33,54].

In addition, findings of increased MD confirm neurodegeneration observed in prior studies. One study found that PD patients with impulse control behaviors (PD-ICB) had higher MD compared to HCs in the UF [35].

5.4. Correlation

Alterations in DTI parameters in PRKN patients were closely linked to both disease duration and serum levels of 9-hydroxystearate, a marker of oxidative stress. The microstructural changes in white matter seen in PRKN patients may therefore be a result of disease duration and oxidative stress. The study by Koinuma et al. [57] showed that the AD values in the UF were negatively correlated with the serum levels of 9-hydroxystearate, while MD and RD values were positively correlated with these levels.

A study found a correlation between the uncinat fasciculus and access to lexical semantic information stored in the temporal lobe, primarily in the left hemisphere. The results suggest that both the right and left UF support word production when selecting among competing alternatives is required [38].

Another study found a significant positive correlation between brain activation in the left IOFC during the verbal learning memory fMRI task and the FA of the right UF. This suggests that the greater the integrity of the UF in PD patients, the greater the functional brain activation in the left IOFC while performing the learning task. The study also revealed a significant correlation between brain activation in the left inferior orbitofrontal cortex (IOFC) during the verbal recognition functional magnetic resonance imaging (fMRI) task and verbal memory impairment, suggesting that the deficit in verbal memory performance during the fMRI paradigm could be influenced by lower brain activation in orbitofrontal cortices during the recognition memory fMRI task [56].

In one study, it was found that there was no relationship between UPDRS and motor scores with the FA of each white matter fasciculus [59].

However, in another study, the FA values were negatively correlated with the UPDRS-III scores across PD patients in the UF [34].

A decrease in total PD-CRS score was associated with decreased FA values in the UF [63]. However, no significant correlation was found between BDI scores and FA values [73].

Additionally, a significant correlation has been observed between the DTI values in the right UF and the Hamilton Depression Scale (HAM-D) scores [66].

In addition, one study found a correlation between MD parameter and MoCa scores in the UF [26].

Based on several studies, the correlation between changes in white matter tracts and cognitive impairment does not seem to be influenced by region, cell type, or gender. Additionally, some studies have reported that voxel-wise correlation analysis for fractional anisotropy (FA) values did not reveal any variations based on either cell type or gender [29].

Further investigation comparing patients with and without Parkinson's disease (PD) found no significant differences in terms of age, gender, or level of education [39]. In addition, the results of multiple linear regression analyses indicated that in people with Parkinson's disease, white matter (WM) integrity and being male were significantly associated with muscle mass [53].

Studies conducted on various diseases, including Alzheimer's disease (AD), have demonstrated that patients may experience changes in brain structure even before displaying symptoms of cognitive impairment [112]. Likewise, the studies we have included suggest that diffusion tensor imaging (DTI) may be useful in detecting microstructural changes in Parkinson's disease before clinical symptoms become apparent [28,29,32,38,39,46,53,58,81,112].

Several studies suggest that in the early stages of Parkinson's disease, neural reorganization may occur as a compensatory mechanism to combat the pathology. This phenomenon could potentially explain why some individuals with Parkinson's disease do not experience cognitive impairments [76].

DTI may not be able to detect early changes in Parkinson's disease, but it can potentially serve as a surrogate marker by differentiating between early and late stages of the disease [45].

To confirm these findings and investigate potential links between preclinical brain changes and later development of cognitive impairment symptoms in Parkinson's disease patients, a longitudinal study is necessary.

Earlier research has suggested that diffusion tensor imaging (DTI) could serve as a diagnostic tool to differentiate Parkinson's disease patients from healthy individuals. By analyzing white matter fiber connections and measuring specific biomarkers, DTI may be capable of providing clinical presentations and assessing the severity of Parkinson's disease [113,114].

As we mentioned before, FA, MD, and other DTI measures could serve as quantitative biomarkers of motor and non-motor symptoms in PD patients. Despite abundant published studies of DTI markers in PD, DTI is not currently widely utilized in clinically standard MRI scanning [115].

Due to limited scanning time, conducting DTI in clinical setting may result in problems such as noise, fiber crossings, low resolution, distortion, and artifacts. Thus, the decreased quality of DTI images makes it hard to obtain precise quantitative measurements [116,117].

The quality of DTI analysis will increase with the use of advanced diffusion techniques, including high-resolution, high-field MRI, enhanced distortion corrections, and fiber crossing solutions [118,119].

However, it is crucial to create clinically useful parameters based on these cutting-edge methods. Furthermore, scanning parameters including MRI field strength, number of encoding directions, and maximum b values have a significant impact on DTI variables. DTI measurements from various MRI facilities need to be harmonized, and consistent

cutoff values for these DTI parameters need to be created in order to eventually improve the individual definition and treatments of PD.

6. Conclusions

Our review provided microstructural insight into the heterogeneous PD subtypes according to their distinct clinically relevant connectivity features.

Cingulum: In this study, we found that individual PD patients had increased MD, possibly defined by degeneration in the early stages. When PD patients experience motor symptoms, FA decreases and/or MD increases, which may result in more degeneration at a later stage of the disease. PD patients with non-motor symptoms showed significant decreases in FA more towards the end of the disease, indicating that extensive degeneration occurred in their non-motor symptoms.

UF: There is a high probability of widespread demyelination and degeneration in UF for PD.

Non-motor symptoms appear lately with extensive degeneration. Cingulum compensation occurred for both motor and non-motor symptoms similarly.

Author Contributions: F.R. and M.H.A. contributed to developing the idea. F.R., Z.K., F.H., M.H.K., N.J. and B.M. contributed to the searching, extraction, and drafting of the manuscript. F.R., M.H.K., F.H. and M.H.A. contributed to editing and revising the manuscript. All authors have read and agreed to the published version of the manuscript.

Funding: We do not have any financial support for this study.

Institutional Review Board Statement: Not applicable.

Informed Consent Statement: Not applicable.

Data Availability Statement: Not applicable.

Acknowledgments: M.H.A. is funded by the EU-project euSNN European School of Network Neuroscience (MSCA-ITN-ETN H2020-860563).

Conflicts of Interest: The authors declare no conflict of interest regarding the publication of this paper.

References

1. Kalia, L.V.; Lang, A. Parkinson's disease. *Lancet* **2015**, *386*, 896–912. [[CrossRef](#)]
2. Dekker, M.C.; Bonifati, V.; van Duijn, C. Parkinson's disease: Piecing together a genetic jigsaw. *Brain* **2003**, *126 Pt 8*, 1722–1733. [[CrossRef](#)] [[PubMed](#)]
3. Grayson, M. Parkinson's disease. *Nature* **2016**, *538*, S1. [[CrossRef](#)]
4. Moustafa, A.A.; Chakravarthy, S.; Phillips, J.R.; Gupta, A.; Keri, S.; Polner, B.; Frank, M.J.; Jahanshahi, M. Motor symptoms in Parkinson's disease: A unified framework. *Neurosci. Biobehav. Rev.* **2016**, *68*, 727–740. [[CrossRef](#)] [[PubMed](#)]
5. Garcia-Ruiz, P.J.; Chaudhuri, K.; Martinez-Martin, P. Non-motor symptoms of Parkinson's disease A review . . . from the past. *J. Neurol. Sci.* **2014**, *338*, 30–33. [[CrossRef](#)] [[PubMed](#)]
6. Zesiewicz, T.A.; Sullivan, K.; Hauser, R. Nonmotor symptoms of Parkinson's disease. *Expert Rev. Neurother.* **2006**, *6*, 1811–1822. [[CrossRef](#)] [[PubMed](#)]
7. Remy, P.; Doder, M.; Lees, A.; Turjanski, N.; Brooks, D. Depression in Parkinson's disease: Loss of dopamine and noradrenaline innervation in the limbic system. *Brain* **2005**, *128 Pt 6*, 1314–1322. [[CrossRef](#)]
8. Todorova, P.; Jenner, P.; Chaudhuri, K.R. Non-motor Parkinson's: Integral to motor Parkinson's, yet often neglected. *Pract. Neurol.* **2014**, *14*, 310–322.
9. Amanollahi, M.; Jameie, M.; Heidari, A.; Rezaei, N. The Dialogue Between Neuroinflammation and Adult Neurogenesis: Mechanisms Involved and Alterations in Neurological Diseases. *Mol. Neurobiol.* **2022**, *60*, 923–959. [[CrossRef](#)]
10. Marxreiter, F.; Regensburger, M.; Winkler, J. Adult neurogenesis in Parkinson's disease. *Cell Mol. Life Sci.* **2013**, *70*, 459–473.
11. Boska, M.D.; Hasan, K.M.; Kibuule, D.; Banerjee, R.; McIntyre, E.; Nelson, J.A.; Hahn, T.; Gendelman, H.E.; Mosley, R.L. Quantitative diffusion tensor imaging detects dopaminergic neuronal degeneration in a murine model of Parkinson's disease. *Neurobiol. Dis.* **2007**, *26*, 590–596. [[CrossRef](#)] [[PubMed](#)]
12. Soria, G.; Aguilar, E.; Tudela, R.; Mullol, J.; Planas, A.M.; Marin, C. In vivo magnetic resonance imaging characterization of bilateral structural changes in experimental Parkinson's disease: A T2 relaxometry study combined with longitudinal diffusion tensor imaging and manganese-enhanced magnetic resonance imaging in the 6-hydroxydopamine rat model. *Eur. J. Neurosci.* **2011**, *33*, 1551–1560. [[PubMed](#)]

13. Huang, P.; Xu, X.; Gu, Q.; Xuan, M.; Yu, X.; Luo, W.; Zhang, M. Disrupted white matter integrity in depressed versus non-depressed Parkinson's disease patients: A tract-based spatial statistics study. *J. Neurol. Sci.* **2014**, *346*, 145–148. [[CrossRef](#)] [[PubMed](#)]
14. Li, W.; Liu, J.; Skidmore, F.; Liu, Y.; Tian, J.; Li, K. White matter microstructure changes in the thalamus in Parkinson disease with depression: A diffusion tensor MR imaging study. *AJNR Am. J. Neuroradiol.* **2010**, *31*, 1861–1866. [[CrossRef](#)]
15. Kötter, R.; Meyer, N. The limbic system: A review of its empirical foundation. *Behav. Brain Res.* **1992**, *52*, 105–127. [[CrossRef](#)]
16. Rajmohan, V.; Mohandas, E. The limbic system. *Indian J. Psychiatry* **2007**, *49*, 132–139. [[CrossRef](#)]
17. Schmahmann, J.D.; Smith, E.E.; Eichler, F.S.; Filley, C.M. Cerebral white matter: Neuroanatomy, clinical neurology, and neurobehavioral correlates. *Ann. N. Y. Acad. Sci.* **2008**, *1142*, 266–309. [[CrossRef](#)]
18. Dalglish, T. The emotional brain. *Nat. Rev. Neurosci.* **2004**, *5*, 583–589. [[CrossRef](#)]
19. Shah, A.; Jhawar, S.S.; Goel, A. Analysis of the anatomy of the Papez circuit and adjoining limbic system by fiber dissection techniques. *J. Clin. Neurosci.* **2012**, *19*, 289–298. [[CrossRef](#)]
20. Bubb, E.J.; Metzler-Baddeley, C.; Aggleton, J.P. The cingulum bundle: Anatomy, function, and dysfunction. *Neurosci. Biobehav. Rev.* **2018**, *92*, 104–127. [[CrossRef](#)]
21. Pierpaoli, C.; Jezzard, P.; Basser, P.J.; Barnett, A.; Di Chiro, G. Diffusion tensor MR imaging of the human brain. *Radiology* **1996**, *201*, 637–648. [[CrossRef](#)] [[PubMed](#)]
22. Tak, H.J.; Kim, J.; Son, S. Developmental process of the arcuate fasciculus from infancy to adolescence: A diffusion tensor imaging study. *Neural Regen. Res.* **2016**, *11*, 937–943. [[PubMed](#)]
23. Alexander, A.L.; Lee, J.E.; Lazar, M.; Field, A.S. Diffusion tensor imaging of the brain. *Neurotherapeutics* **2007**, *4*, 316–329. [[CrossRef](#)] [[PubMed](#)]
24. Xu, Q.; Park, Y.; Huang, X.; Hollenbeck, A.; Blair, A.; Schatzkin, A.; Chen, H. Physical activities and future risk of Parkinson disease. *Neurology* **2010**, *75*, 341–348. [[CrossRef](#)]
25. Mole, J.P.; Subramanian, L.; Bracht, T.; Morris, H.; Metzler-Baddeley, C.; Linden, D.E. Increased fractional anisotropy in the motor tracts of Parkinson's disease suggests compensatory neuroplasticity or selective neurodegeneration. *Eur. Radiol.* **2016**, *26*, 3327–3335. [[CrossRef](#)] [[PubMed](#)]
26. Chen, B.; Fan, G.G.; Liu, H.; Wang, S. Changes in anatomical and functional connectivity of Parkinson's disease patients according to cognitive status. *Eur. J. Radiol.* **2015**, *84*, 1318–1324. [[CrossRef](#)]
27. Li, Z.; Liu, W.; Xiao, C.; Wang, X.; Zhang, X.; Yu, M.; Hu, X.; Qian, L. Abnormal white matter microstructures in Parkinson's disease and comorbid depression: A whole-brain diffusion tensor imaging study. *Neurosci. Lett.* **2020**, *735*, 135238. [[CrossRef](#)]
28. Holtbernd, F.; Romanzetti, S.; Oertel, W.H.; Knake, S.; Sittig, E.; Heidebreder, A.; Maier, A.; Krahe, J.; Wojtala, J.; Dogan, I. Convergent patterns of structural brain changes in rapid eye movement sleep behavior disorder and Parkinson's disease on behalf of the German rapid eye movement sleep behavior disorder study group. *Sleep* **2021**, *44*, zsa199. [[CrossRef](#)]
29. Gorges, M.; Müller, H.-P.; Liepelt-Scarfone, I.; Storch, A.; Dodel, R.; Consortium, L.; Hilker-Roggenendorf, R.; Berg, D.; Kunz, M.S.; Kalbe, E. Structural brain signature of cognitive decline in Parkinson's disease: DTI-based evidence from the LANDSCAPE study. *Ther. Adv. Neurol. Disord.* **2019**, *12*, 1756286419843447. [[CrossRef](#)]
30. Sun, J.; Chen, R.; Tong, Q.; Ma, J.; Gao, L.; Fang, J.; Zhang, D.; Chan, P.; He, H.; Wu, T. Convolutional neural network optimizes the application of diffusion kurtosis imaging in Parkinson's disease. *Brain Inform.* **2021**, *8*, 1–12. [[CrossRef](#)]
31. Jalakas, M.; Palmqvist, S.; Hall, S.; Svård, D.; Lindberg, O.; Pereira, J.B.; van Westen, D.; Hansson, O. A quick test of cognitive speed can predict development of dementia in Parkinson's disease. *Sci. Rep.* **2019**, *9*, 15417. [[CrossRef](#)]
32. Andica, C.; Kamagata, K.; Hatano, T.; Saito, A.; Uchida, W.; Ogawa, T.; Takeshige-Amano, H.; Zalesky, A.; Wada, A.; Suzuki, M. Free-water imaging in white and gray matter in Parkinson's disease. *Cells* **2019**, *8*, 839. [[CrossRef](#)]
33. Andica, C.; Kamagata, K.; Hatano, T.; Saito, Y.; Uchida, W.; Ogawa, T.; Takeshige-Amano, H.; Hagiwara, A.; Murata, S.; Oyama, G. Neurocognitive and psychiatric disorders-related axonal degeneration in Parkinson's disease. *J. Neurosci. Res.* **2020**, *98*, 936–949. [[CrossRef](#)] [[PubMed](#)]
34. Chen, N.-K.; Chou, Y.-H.; Sundman, M.; Hickey, P.; Kasoff, W.S.; Bernstein, A.; Trouard, T.P.; Lin, T.; Rapcsak, S.Z.; Sherman, S.J. Alteration of diffusion-tensor magnetic resonance imaging measures in brain regions involved in early stages of parkinson's disease. *Brain Connect.* **2018**, *8*, 343–349. [[CrossRef](#)] [[PubMed](#)]
35. Takeshige-Amano, H.; Hatano, T.; Kamagata, K.; Andica, C.; Uchida, W.; Abe, M.; Ogawa, T.; Shimo, Y.; Oyama, G.; Umemura, A. White matter microstructures in Parkinson's disease with and without impulse control behaviors. *Ann. Clin. Transl. Neurol.* **2022**, *9*, 253–263. [[CrossRef](#)]
36. Wu, J.Y.; Zhang, Y.; Wu, W.B.; Hu, G.; Xu, Y. Impaired long contact white matter fibers integrity is related to depression in Parkinson's disease. *CNS Neurosci. Ther.* **2018**, *24*, 108–114. [[CrossRef](#)]
37. Chen, J.; Jiang, X.; Wu, J.; Wu, H.; Zhou, C.; Guo, T.; Bai, X.; Liu, X.; Wen, J.; Cao, Z. Gray and white matter alterations in different predominant side and type of motor symptom in Parkinson's disease. *CNS Neurosci. Ther.* **2022**, *28*, 1372–1379. [[CrossRef](#)] [[PubMed](#)]
38. Di Tella, S.; Baglio, F.; Pelizzari, L.; Cabinio, M.; Nemni, R.; Traficante, D.; Silveri, M.C. Uncinate fasciculus and word selection processing in Parkinson's disease. *Neuropsychologia* **2020**, *146*, 107504. [[CrossRef](#)]
39. Duncan, G.W.; Firbank, M.J.; Yarnall, A.J.; Khoo, T.K.; Brooks, D.J.; Barker, R.A.; Burn, D.J.; O'Brien, J.T. Gray and white matter imaging: A biomarker for cognitive impairment in early P arkinson's disease? *Mov. Disord.* **2016**, *31*, 103–110. [[CrossRef](#)]

40. Lenka, A.; Ingalthalika, M.; Shah, A.; Saini, J.; Arumugham, S.S.; Hegde, S.; George, L.; Yadav, R.; Pal, P.K. Abnormalities in the white matter tracts in patients with Parkinson disease and psychosis. *Neurology* **2020**, *94*, e1876–e1884. [[CrossRef](#)]
41. Patriat, R.; Pisharady, P.K.; Amundsen-Huffmaster, S.; Linn-Evans, M.; Howell, M.; Chung, J.W.; Petrucci, M.N.; Videnovic, A.; Holker, E.; De Kam, J. White matter microstructure in Parkinson's disease with and without elevated rapid eye movement sleep muscle tone. *Brain Commun.* **2022**, *4*, fcac027. [[CrossRef](#)]
42. Feng, Y.; Yan, W.; Wang, J.; Song, J.; Zeng, Q.; Zhao, C. Local white matter fiber clustering differentiates Parkinson's disease diagnoses. *Neuroscience* **2020**, *435*, 146–160. [[CrossRef](#)]
43. Nilsson, M.; Szczepankiewicz, F.; van Westen, D.; Hansson, O. Extrapolation-based references improve motion and eddy-current correction of high B-value DWI data: Application in Parkinson's disease dementia. *PLoS ONE* **2015**, *10*, e0141825. [[CrossRef](#)] [[PubMed](#)]
44. Gou, L.; Zhang, W.; Li, C.; Shi, X.; Zhou, Z.; Zhong, W.; Chen, T.; Wu, X.; Yang, C.; Guo, D. Structural brain network alteration and its correlation with structural impairments in patients with depression in de novo and drug-naïve Parkinson's disease. *Front. Neurol.* **2018**, *9*, 608. [[CrossRef](#)] [[PubMed](#)]
45. Guimarães, R.P.; Campos, B.M.; de Rezende, T.J.; Piovesana, L.; Azevedo, P.C.; Amato-Filho, A.C.; Cendes, F.; D'Abreu, A. Is diffusion tensor imaging a good biomarker for early Parkinson's disease? *Front. Neurol.* **2018**, *9*, 626. [[CrossRef](#)] [[PubMed](#)]
46. Jin, C.; Qi, S.; Teng, Y.; Li, C.; Yao, Y.; Ruan, X.; Wei, X. Integrating structural and functional interhemispheric brain connectivity of gait freezing in Parkinson's disease. *Front. Neurol.* **2021**, *12*, 609866. [[CrossRef](#)] [[PubMed](#)]
47. Yang, Y.; Yang, Y.; Pan, A.; Xu, Z.; Wang, L.; Zhang, Y.; Nie, K.; Huang, B. Identifying Depression in Parkinson's Disease by Using Combined Diffusion Tensor Imaging and Support Vector Machine. *Front. Neurol.* **2022**, *13*, 878691. [[CrossRef](#)] [[PubMed](#)]
48. Guan, X.; Huang, P.; Zeng, Q.; Liu, C.; Wei, H.; Xuan, M.; Gu, Q.; Xu, X.; Wang, N.; Yu, X. Quantitative susceptibility mapping as a biomarker for evaluating white matter alterations in Parkinson's disease. *Brain Imaging Behav.* **2019**, *13*, 220–231. [[CrossRef](#)]
49. Canu, E.; Agosta, F.; Sarasso, E.; Volonte, M.A.; Basaia, S.; Stojkovic, T.; Stefanova, E.; Comi, G.; Falini, A.; Kostic, V.S. Brain structural and functional connectivity in Parkinson's disease with freezing of gait. *Hum. Brain Mapp.* **2015**, *36*, 5064–5078. [[CrossRef](#)]
50. Ji, G.J.; Ren, C.; Li, Y.; Sun, J.; Liu, T.; Gao, Y.; Xue, D.; Shen, L.; Cheng, W.; Zhu, C. Regional and network properties of white matter function in Parkinson's disease. *Hum. Brain Mapp.* **2019**, *40*, 1253–1263. [[CrossRef](#)]
51. Guo, T.; Guan, X.; Zhou, C.; Gao, T.; Wu, J.; Song, Z.; Xuan, M.; Gu, Q.; Huang, P.; Pu, J. Clinically relevant connectivity features define three subtypes of Parkinson's disease patients. *Hum. Brain Mapp.* **2020**, *41*, 4077–4092. [[CrossRef](#)]
52. Xiao, Y.; Peters, T.M.; Khan, A.R. Characterizing white matter alterations subject to clinical laterality in drug-naïve de novo Parkinson's disease. *Hum. Brain Mapp.* **2021**, *42*, 4465–4477. [[CrossRef](#)]
53. Lee, C.-Y.; Chen, H.-L.; Chen, P.-C.; Chen, Y.-S.; Chiang, P.-L.; Wang, C.-K.; Lu, C.-H.; Chen, M.-H.; Chou, K.-H.; Huang, Y.-C. Correlation between executive network integrity and sarcopenia in patients with Parkinson's disease. *Int. J. Environ. Res. Public Health* **2019**, *16*, 4884. [[CrossRef](#)] [[PubMed](#)]
54. Imperiale, F.; Agosta, F.; Canu, E.; Markovic, V.; Inuggi, A.; Jecmenica-Lukic, M.; Tomic, A.; Copetti, M.; Basaia, S.; Kostic, V. Brain structural and functional signatures of impulsive-compulsive behaviours in Parkinson's disease. *Mol. Psychiatry* **2018**, *23*, 459–466. [[CrossRef](#)] [[PubMed](#)]
55. Yoo, H.B.; Lee, J.-Y.; Lee, J.S.; Kang, H.; Kim, Y.K.; Song, I.C.; Lee, D.S.; Jeon, B.S. Whole-brain diffusion-tensor changes in parkinsonian patients with impulse control disorders. *J. Clin. Neurol.* **2015**, *11*, 42–47. [[CrossRef](#)]
56. Lucas-Jiménez, O.; Diez-Cirarda, M.; Ojeda, N.; Pena, J.; Cabrera-Zubizarreta, A.; Ibarretxe-Bilbao, N. Verbal memory in parkinson's disease: A combined DTI and fMRI study. *J. Park. Dis.* **2015**, *5*, 793–804. [[CrossRef](#)] [[PubMed](#)]
57. Koinuma, T.; Hatano, T.; Kamagata, K.; Andica, C.; Mori, A.; Ogawa, T.; Takeshige-Amano, H.; Uchida, W.; Saiki, S.; Okuzumi, A. Diffusion MRI Captures White Matter Microstructure Alterations in PRKN Disease. *J. Park. Dis.* **2021**, *11*, 1221–1235. [[CrossRef](#)]
58. Georgiopoulos, C.; Warntjes, M.; Dizdar, N.; Zachrisson, H.; Engström, M.; Haller, S.; Larsson, E.-M. Olfactory impairment in Parkinson's disease studied with diffusion tensor and magnetization transfer imaging. *J. Park. Dis.* **2017**, *7*, 301–311. [[CrossRef](#)]
59. Li, X.-R.; Ren, Y.-D.; Cao, B.; Huang, X.-L. Analysis of white matter characteristics with tract-based spatial statistics according to diffusion tensor imaging in early Parkinson's disease. *Neurosci. Lett.* **2018**, *675*, 127–132. [[CrossRef](#)] [[PubMed](#)]
60. Akio, H.; Togao, O.; Yamashita, K.; Somehara, R.; Kamei, R.; Baba, S. Structural changes in Parkinson's disease: Voxel-based morphometry and diffusion tensor imaging analyses based on 123I-MIBG uptake. *Eur. Radiol.* **2017**, *27*, 5073–5079.
61. Mishra, V.R.; Sreenivasan, K.R.; Zhuang, X.; Yang, Z.; Cordes, D.; Walsh, R.R. Influence of analytic techniques on comparing DTI-derived measurements in early stage Parkinson's disease. *Heliyon* **2019**, *5*, e01481. [[CrossRef](#)] [[PubMed](#)]
62. Minett, T.; Su, L.; Mak, E.; Williams, G.; Firbank, M.; Lawson, R.A.; Yarnall, A.J.; Duncan, G.W.; Owen, A.M.; Khoo, T.K. Longitudinal diffusion tensor imaging changes in early Parkinson's disease: ICICLE-PD study. *J. Neurol.* **2018**, *265*, 1528–1539. [[CrossRef](#)] [[PubMed](#)]
63. Chondrogiorgi, M.; Astrakas, L.G.; Zikou, A.K.; Weis, L.; Xydis, V.G.; Antonini, A.; Argyropoulou, M.I.; Konitsiotis, S. Multifocal alterations of white matter accompany the transition from normal cognition to dementia in Parkinson's disease patients. *Brain Imaging Behav.* **2019**, *13*, 232–240. [[CrossRef](#)] [[PubMed](#)]
64. Koshimori, Y.; Segura, B.; Christopher, L.; Lobaugh, N.; Duff-Canning, S.; Mizrahi, R.; Hamani, C.; Lang, A.E.; Aminian, K.; Houle, S. Imaging changes associated with cognitive abnormalities in Parkinson's disease. *Brain Struct. Funct.* **2015**, *220*, 2249–2261. [[CrossRef](#)] [[PubMed](#)]

65. Jiang, M.-f.; Shi, F.; Niu, G.-m.; Xie, S.-h.; Yu, S.-y. A novel method for evaluating brain function and microstructural changes in Parkinson's disease. *Neural Regen. Res.* **2015**, *10*, 2025. [[PubMed](#)]
66. Pietracupa, S.; Suppa, A.; Upadhyay, N.; Gianni, C.; Grillea, G.; Leodori, G.; Modugno, N.; Di Biasio, F.; Zampogna, A.; Colonnese, C. Freezing of gait in Parkinson's disease: Gray and white matter abnormalities. *J. Neurol.* **2018**, *265*, 52–62. [[CrossRef](#)]
67. Inguanzo, A.; Sala-Llonch, R.; Segura, B.; Erostarbe, H.; Abós, A.; Campabadal, A.; Uribe, C.; Baggio, H.C.; Compta, Y.; Martí, M. Hierarchical cluster analysis of multimodal imaging data identifies brain atrophy and cognitive patterns in Parkinson's disease. *Park. Relat. Disord.* **2021**, *82*, 16–23. [[CrossRef](#)]
68. Pelizzari, L.; Di Tella, S.; Laganà, M.M.; Bergsland, N.; Rossetto, F.; Nemni, R.; Baglio, F. White matter alterations in early Parkinson's disease: Role of motor symptom lateralization. *Neurol. Sci.* **2020**, *41*, 357–364. [[CrossRef](#)]
69. Melzer, T.R.; Myall, D.J.; MacAskill, M.R.; Pitcher, T.L.; Livingston, L.; Watts, R.; Keenan, R.J.; Dalrymple-Alford, J.C.; Anderson, T.J. Tracking Parkinson's disease over one year with multimodal magnetic resonance imaging in a group of older patients with moderate disease. *PLoS ONE* **2015**, *10*, e0143923. [[CrossRef](#)] [[PubMed](#)]
70. Surova, Y.; Lampinen, B.; Nilsson, M.; Lätt, J.; Hall, S.; Widner, H.; Swedish BioFINDER Study; van Westen, D.; Hansson, O. Alterations of diffusion kurtosis and neurite density measures in deep grey matter and white matter in Parkinson's disease. *PLoS ONE* **2016**, *11*, e0157755. [[CrossRef](#)]
71. Ogawa, T.; Hatano, T.; Kamagata, K.; Andica, C.; Takeshige-Amano, H.; Uchida, W.; Saito, Y.; Shimo, Y.; Oyama, G.; Umemura, A. White matter alterations in Parkinson's disease with levodopa-induced dyskinesia. *Park. Relat. Disord.* **2021**, *90*, 8–14. [[CrossRef](#)] [[PubMed](#)]
72. Yu, J.; Chen, L.; Cai, G.; Wang, Y.; Chen, X.; Hong, W.; Ye, Q. Evaluating white matter alterations in Parkinson's disease-related parkin S/N167 mutation carriers using tract-based spatial statistics. *Quant. Imaging Med. Surg.* **2022**, *12*, 4272. [[CrossRef](#)]
73. Shen, Q.; Liu, Y.; Guo, J.; Zhang, H.; Xiang, Y.; Liao, H.; Cai, S.; Zhou, B.; Wang, M.; Liu, S. Impaired white matter microstructure associated with severe depressive symptoms in patients with PD. *Brain Imaging Behav.* **2022**, *16*, 169–175. [[CrossRef](#)]
74. Seki, M.; Seppi, K.; Mueller, C.; Potrusil, T.; Goebel, G.; Reiter, E.; Nocker, M.; Kremser, C.; Wildauer, M.; Schocke, M. Diagnostic potential of multimodal MRI markers in atypical parkinsonian disorders. *J. Park. Dis.* **2019**, *9*, 681–691. [[CrossRef](#)] [[PubMed](#)]
75. Wang, M.; Jiang, S.; Yuan, Y.; Zhang, L.; Ding, J.; Wang, J.; Zhang, J.; Zhang, K.; Wang, J. Alterations of functional and structural connectivity of freezing of gait in Parkinson's disease. *J. Neurol.* **2016**, *263*, 1583–1592. [[CrossRef](#)]
76. Wen, M.-C.; Heng, H.S.; Lu, Z.; Xu, Z.; Chan, L.L.; Tan, E.K.; Tan, L.C. Differential white matter regional alterations in motor subtypes of early drug-naive Parkinson's disease patients. *Neurorehabilit. Neural Repair* **2018**, *32*, 129–141. [[CrossRef](#)] [[PubMed](#)]
77. Wang, J.; Zhang, F.; Zhao, C.; Zeng, Q.; He, J.; O'Donnell, L.J.; Feng, Y. Investigation of local white matter abnormality in Parkinson's disease by using an automatic fiber tract parcellation. *Behav. Brain Res.* **2020**, *394*, 112805. [[CrossRef](#)]
78. Zhang, Y.; Wu, J.; Wu, W.; Liu, R.; Pang, L.; Guan, D.; Xu, Y. Reduction of white matter integrity correlates with apathy in Parkinson's disease. *Int. J. Neurosci.* **2018**, *128*, 25–31. [[CrossRef](#)]
79. Chen, M.-H.; Chen, P.-C.; Lu, C.-H.; Chen, H.-L.; Chao, Y.-P.; Li, S.-H.; Chen, Y.-W.; Lin, W.-C. Plasma DNA mediate autonomic dysfunctions and white matter injuries in patients with Parkinson's disease. *Oxidative Med. Cell. Longev.* **2017**, *2017*, 7371403. [[CrossRef](#)]
80. Chen, F.; Wu, T.; Luo, Y.; Li, Z.; Guan, Q.; Meng, X.; Tao, W.; Zhang, H. Amnesic mild cognitive impairment in Parkinson's disease: White matter structural changes and mechanisms. *PLoS ONE* **2019**, *14*, e0226175. [[CrossRef](#)]
81. Lu, C.-S.; Ng, S.-H.; Weng, Y.-H.; Cheng, J.-S.; Lin, W.-Y.; Wai, Y.-Y.; Chen, Y.-L.; Wang, J.-J. Alterations of diffusion tensor MRI parameters in the brains of patients with Parkinson's disease compared with normal brains: Possible diagnostic use. *Eur. Radiol.* **2016**, *26*, 3978–3988. [[CrossRef](#)] [[PubMed](#)]
82. Zhou, W.; Jiang, J.; Peng, W.; Zhou, X.; Du, J.; Mo, L.; Tan, C.; Liu, X.; Chen, L. Levodopa responsiveness in Parkinson's disease patients and white matter alterations in diffusion tensor imaging: A cross-sectional tract-based spatial statistics study. *NeuroReport* **2021**, *32*, 636–642. [[CrossRef](#)] [[PubMed](#)]
83. Ansari, M.; Rahmani, F.; Dolatshahi, M.; Pooyan, A.; Aarabi, M.H. Brain pathway differences between Parkinson's disease patients with and without REM sleep behavior disorder. *Sleep Breath.* **2017**, *21*, 155–161. [[CrossRef](#)]
84. Kang, S.Y.; Bang, M.; Hong, J.Y.; Oh, J.; Kim, J.S.; Han, Y.M.; Chang, S.K.; Lee, S.A.; Yoon, U.; Shin, N.-Y. Neural and dopaminergic correlates of fatigue in Parkinson's disease. *J. Neural Transm.* **2020**, *127*, 301–309. [[CrossRef](#)] [[PubMed](#)]
85. Uhr, L.; Tsolaki, E.; Pouratian, N. Diffusion tensor imaging correlates of depressive symptoms in Parkinson disease. *J. Comp. Neurol.* **2022**, *530*, 1729–1738. [[CrossRef](#)]
86. Zhang, Z.; Liao, M.; Yao, Z.; Hu, B.; Xie, Y.; Zheng, W.; Hu, T.; Zhao, Y.; Yang, F.; Zhang, Y. Frequency-specific functional connectivity density as an effective biomarker for adolescent generalized anxiety disorder. *Front. Hum. Neurosci.* **2017**, *11*, 549. [[CrossRef](#)]
87. Acosta-Cabronero, J.; Williams, G.B.; Pengas, G.; Nestor, P.J. Absolute diffusivities define the landscape of white matter degeneration in Alzheimer's disease. *Brain* **2010**, *133*, 529–539. [[CrossRef](#)]
88. Curran, K.M.; Emsell, L.; Leemans, A. Quantitative DTI measures. *Diffus. Tensor Imaging A Pract. Handb.* **2016**, 65–87. [[CrossRef](#)]
89. Chu, Y.; Morfini, G.A.; Langhamer, L.B.; He, Y.; Brady, S.T.; Kordower, J.H. Alterations in axonal transport motor proteins in sporadic and experimental Parkinson's disease. *Brain* **2012**, *135 Pt 7*, 2058–2073. [[CrossRef](#)]
90. Sanjari Moghaddam, H.; Dolatshahi, M.; Salardini, E.; Aarabi, M.H. Association of olfaction dysfunction with brain microstructure in prodromal Parkinson disease. *Neurol. Sci.* **2019**, *40*, 283–291. [[CrossRef](#)]

91. Ghazi Sherbaf, F.; Rostam Abadi, Y.; Mojtahed Zadeh, M.; Ashraf-Ganjouei, A.; Sanjari Moghaddam, H.; Aarabi, M.H. Microstructural changes in patients with Parkinson's disease comorbid with REM sleep behaviour disorder and depressive symptoms. *Front. Neurol.* **2018**, *9*, 441. [[CrossRef](#)]
92. Ghazi Sherbaf, F.; Rahmani, F.; Jooyandeh, S.M.; Aarabi, M.H. Microstructural changes in patients with Parkinson disease and REM sleep behavior disorder: Depressive symptoms versus non-depressed. *Acta Neurol. Belg.* **2018**, *118*, 415–421. [[CrossRef](#)]
93. Sobhani, S.; Rahmani, F.; Aarabi, M.H.; Sadr, A.V. Exploring white matter microstructure and olfaction dysfunction in early parkinson disease: Diffusion MRI reveals new insight. *Brain Imaging Behav.* **2019**, *13*, 210–219. [[CrossRef](#)]
94. Song, S.-K.; Sun, S.-W.; Ju, W.-K.; Lin, S.-J.; Cross, A.H.; Neufeld, A.H. Diffusion tensor imaging detects and differentiates axon and myelin degeneration in mouse optic nerve after retinal ischemia. *Neuroimage* **2003**, *20*, 1714–1722. [[CrossRef](#)]
95. Sun, S.-W.; Song, S.-K.; Harms, M.P.; Lin, S.-J.; Holtzman, D.M.; Merchant, K.M.; Kotyk, J.J. Detection of age-dependent brain injury in a mouse model of brain amyloidosis associated with Alzheimer's disease using magnetic resonance diffusion tensor imaging. *Exp. Neurol.* **2005**, *191*, 77–85. [[CrossRef](#)] [[PubMed](#)]
96. Gudala, K.; Bansal, D.; Muthyala, H. Role of serum cholesterol in Parkinson's disease: A meta-analysis of evidence. *J. Park. Dis.* **2013**, *3*, 363–370. [[CrossRef](#)]
97. Rahmani, F.; Aarabi, M.H. Does apolipoprotein A1 predict microstructural changes in subgenual cingulum in early Parkinson? *J. Neurol.* **2017**, *264*, 684–693. [[CrossRef](#)]
98. Von Der Heide, R.J.; Skipper, L.M.; Klobusicky, E.; Olson, I.R. Dissecting the uncinat fasciculus: Disorders, controversies and a hypothesis. *Brain* **2013**, *136*, 1692–1707. [[CrossRef](#)] [[PubMed](#)]
99. Kitada, T.; Asakawa, S.; Hattori, N.; Matsumine, H.; Yamamura, Y.; Minoshima, S.; Yokochi, M.; Mizuno, Y.; Shimizu, N. Mutations in the parkin gene cause autosomal recessive juvenile parkinsonism. *Nature* **1998**, *392*, 605–608. [[CrossRef](#)] [[PubMed](#)]
100. Concha, L. A macroscopic view of microstructure: Using diffusion-weighted images to infer damage, repair, and plasticity of white matter. *Neuroscience* **2014**, *276*, 14–28. [[CrossRef](#)]
101. Tighe, S.K.; Oishi, K.; Mori, S.; Smith, G.S.; Albert, M.; Lyketsos, C.G.; Mielke, M.M. Diffusion tensor imaging of neuropsychiatric symptoms in mild cognitive impairment and Alzheimer's dementia. *J. Neuropsychiatry Clin. Neurosci.* **2012**, *24*, 484–488. [[CrossRef](#)] [[PubMed](#)]
102. Nagasaka, K.; Watanabe, Y.; Takashima, I. Topographical projections from the nucleus basalis magnocellularis (Meynert) to the frontal cortex: A voltage-sensitive dye imaging study in rats. *Brain Stimul.* **2017**, *10*, 977–980. [[CrossRef](#)] [[PubMed](#)]
103. Biundo, R.; Weis, L.; Antonini, A. Cognitive decline in Parkinson's disease: The complex picture. *Npj Park. Dis.* **2016**, *2*, 1–7. [[CrossRef](#)]
104. Schapira, A.H.; Chaudhuri, K.; Jenner, P. Non-motor features of Parkinson disease. *Nat. Rev. Neurosci.* **2017**, *18*, 435–450. [[CrossRef](#)]
105. Delaville, C.; Deurwaerdère, P.D.; Benazzouz, A. Noradrenaline and Parkinson's disease. *Front. Syst. Neurosci.* **2011**, *5*, 31. [[CrossRef](#)]
106. Perez-Lloret, S.; Barrantes, F.J. Deficits in cholinergic neurotransmission and their clinical correlates in Parkinson's disease. *Npj Park. Dis.* **2016**, *2*, 1–12. [[CrossRef](#)] [[PubMed](#)]
107. De Kwaasteniet, B.; Ruhe, E.; Caan, M.; Rive, M.; Olabarriaga, S.; Groefsema, M.; Heesink, L.; van Wingen, G.; Denys, D. Relation between structural and functional connectivity in major depressive disorder. *Biol. Psychiatry* **2013**, *74*, 40–47. [[CrossRef](#)]
108. Delaparte, L.; Yeh, F.-C.; Adams, P.; Malchow, A.; Trivedi, M.H.; Oquendo, M.A.; Deckersbach, T.; Ogden, T.; Pizzagalli, D.A.; Fava, M. A comparison of structural connectivity in anxious depression versus non-anxious depression. *J. Psychiatr. Res.* **2017**, *89*, 38–47. [[CrossRef](#)] [[PubMed](#)]
109. Hettema, J.M.; Kettenmann, B.; Ahluwalia, V.; McCarthy, C.; Kates, W.R.; Schmitt, J.E.; Silberg, J.L.; Neale, M.C.; Kendler, K.S.; Fatouros, P. Pilot multimodal twin imaging study of generalized anxiety disorder. *Depress. Anxiety* **2012**, *29*, 202–209. [[CrossRef](#)]
110. Feldman, H.M.; Yeatman, J.D.; Lee, E.S.; Barde, L.H.; Gaman-Bean, S. Diffusion tensor imaging: A review for pediatric researchers and clinicians. *J. Dev. Behav. Pediatr. JDBP* **2010**, *31*, 346. [[CrossRef](#)]
111. Alexander, A.L.; Hurley, S.A.; Samsonov, A.A.; Adluru, N.; Hosseinbor, A.P.; Mossahebi, P.; Tromp, D.P.; Zakszewski, E.; Field, A.S. Characterization of cerebral white matter properties using quantitative magnetic resonance imaging stains. *Brain Connect.* **2011**, *1*, 423–446. [[CrossRef](#)] [[PubMed](#)]
112. Avila Villanueva, M.; Marcos Dolado, A.; Gomez Ramirez, J.; Fernandez-Blazquez, M.A. Brain structural and functional changes in cognitive impairment due to Alzheimer's disease. *Front. Psychol.* **2022**, *13*, 886619. [[CrossRef](#)] [[PubMed](#)]
113. Cochrane, C.J.; Ebmeier, K.P. Diffusion tensor imaging in parkinsonian syndromes: A systematic review and meta-analysis. *Neurology* **2013**, *80*, 857–864. [[CrossRef](#)]
114. Ofori, E.; Pasternak, O.; Planetta, P.J.; Li, H.; Burciu, R.G.; Snyder, A.F.; Lai, S.; Okun, M.S.; Vaillancourt, D.E. Longitudinal changes in free-water within the substantia nigra of Parkinson's disease. *Brain* **2015**, *138*, 2322–2331. [[CrossRef](#)]
115. Zhang, Y. and M.A. Burock, Diffusion tensor imaging in Parkinson's disease and parkinsonian syndrome: A systematic review. *Front. Neurol.* **2020**, *11*, 531993. [[CrossRef](#)]
116. Bergamino, M.; Keeling, E.G.; Mishra, V.R.; Stokes, A.M.; Walsh, R.R. Assessing white matter pathology in early-stage Parkinson disease using diffusion MRI: A systematic review. *Front. Neurol.* **2020**, *11*, 314. [[CrossRef](#)]

117. Atkinson-Clement, C.; Pinto, S.; Eusebio, A.; Coulon, O. Diffusion tensor imaging in Parkinson's disease: Review and meta-analysis. *NeuroImage Clin.* **2017**, *16*, 98–110. [[CrossRef](#)] [[PubMed](#)]
118. Tuch, D.S.; Reese, T.G.; Wiegell, M.R.; Makris, N.; Belliveau, J.W.; Wedeen, V.J. High angular resolution diffusion imaging reveals intravoxel white matter fiber heterogeneity. *Magn. Reson. Med. Off. J. Int. Soc. Magn. Reson. Med.* **2002**, *48*, 577–582. [[CrossRef](#)]
119. Wedeen, V.J.; Wang, R.; Schmahmann, J.D.; Benner, T.; Tseng, W.-Y.I.; Dai, G.; Pandya, D.; Hagmann, P.; D'Arceuil, H.; de Crespigny, A.J. Diffusion spectrum magnetic resonance imaging (DSI) tractography of crossing fibers. *Neuroimage* **2008**, *41*, 1267–1277. [[CrossRef](#)]

Disclaimer/Publisher's Note: The statements, opinions and data contained in all publications are solely those of the individual author(s) and contributor(s) and not of MDPI and/or the editor(s). MDPI and/or the editor(s) disclaim responsibility for any injury to people or property resulting from any ideas, methods, instructions or products referred to in the content.